50272-101

REPORT DOCUMENTATION PAGE	1. REPORT NO. NSF/RA-790130	2.	3. Recipient's Accession No. PB301369

4. Title and Subtitle

Probabilistic Model for Seismic Slope Stability Analysis

5. Report Date June, 1979

6.

7. Author(s)

D. A-Grivas, J. Howland, P. Tolcser

8. Performing Organization Rept. No. CE-78-5

9. Performing Organization Name and Address

Rensselaer Polytechnic Institute
Department of Civil Engineering
Troy, New York 12181

10. Project/Task/Work Unit No.

11. Contract(C) or Grant(G) No.

(C)

(G) ENV7716185

12. Sponsoring Organization Name and Address

Engineering and Applied Science (EAS)
National Science Foundation
1800 G Street, N.W.
Washington, D.C. 20550

13. Type of Report & Period Covered

14.

15. Supplementary Notes

16. Abstract (Limit: 200 words)

A model for probabilistic stability analysis of earth slopes under earthquake loading is presented. Significant uncertainties associated with conventional pseudo-static methods of seismic stability analysis are recognized and probabilistic tools are introduced for their description and amelioration. The proposed method of analysis accounts for: the variability of material strength parameters; the uncertainty in the exact location of potential failure surfaces; and the uncertainty in the value of the maximum slope acceleration during an earthquake. The soil material comprised in the slope is assumed to be probabilistically homogeneous with strength parameters being identically distributed random variables with given statistical values. Potential failure surfaces are considered to have an exponential shape defined with the aid of three random variables. Slope safety is measured in terms of its probability of failure. The seismic load is introduced into the analysis through the maximum horizontal acceleration experienced by the slope during an earthquake. Two different attenuation relationships are employed to determine the maximum horizontal ground acceleration and the corresponding results are compared and discussed.

17. Document Analysis a. Descriptors

Models	Loading
Seismology	Loads
Earthquakes	Mathematical prediction

b. Identifiers/Open-Ended Terms

Structural loading
Seismic stability analysis

c. COSATI Field/Group

18. Availability Statement

NTIS

19. Security Class (This Report)

20. Security Class (This Page)

22. Price MF-A01 PC A05

A PROBABILISTIC MODEL FOR SEISMIC

SLOPE STABILITY ANALYSIS

by

D. A-Grivas, J. Howland, and P. Tolcser

Report No. CE-78-5

Department of Civil Engineering
Rensselaer Polytechnic Institute
Troy, N.Y. 12181

Sponsored by the National Science Foundation (ASRA)

Grant No. ENV 77-16185

June 1979

TABLE OF CONTENTS

PREFACE

This the first in a series of reports on a project under the general title "Reliability Analysis of Soil Slopes During Earthquakes". This study is sponsored by the Earthquake Hazard Mitigation Program of the National Science Foundation (ASRA) under Grant No. ENV 77-16185. Dr. Michael Gaus is the program manager of this project of which the first author is the principal investigator.

Three reports of this series, although not issued simultaneously, compose a unity in content. These are the following:

(1) Report No. CE-78-5 entitled "A Probabilistic Model for Seismic Slope Stability Analysis", June 1979.

(2) Report No. CE-78-6 entitled "Program RASSUEL - Reliability Analysis of Soil Slopes Under Earthquake Loading", December 1978.

(3) Report No. CE-79-1 entitled "Probabilistic Seismic Stability Analysis - A Case Study", July 1979.

The first of these reports presents the model and discusses its applicability and limitations. The second is a document pertaining to the computer program "RASSUEL" that has been developed to perform the probabilistic seismic stability analysis; it provides a description of the various functions and options available in the program as well as guidelines for its use. Finally, the third report presents the results of a case study involving the assessment of the safety of a natural slope located near Slingerlands, New York.

The authors wish to thank the National Science Foundation for sponsoring this study. As a Monte Carlo simulation of the failure of slopes was originally pursued by the first author during his doctoral studies at Purdue University, he is indebted to Professors M.E. Harr and J.T.P. Yao for their assistance in formulating the problem. The help of Messrs. R. Dyvik and G. Nadeau is acknowledged. Appreciation also goes to Professor R. Dobry for his useful comments. Finally, special thanks are extended to Mrs. Betty Alix for her excellent typing of this report.

LIST OF FIGURES

LIST OF FIGURES (continued)

LIST OF TABLES

LIST OF SYMBOLS

English Characters

a_{max}	Maximum horizontal ground acceleration at the slope site (random variable)
b_i	Regional parameters for the attenuation relations (i=1 to 4)
c	Soil strength parameter (random variable)
D,d	Distance
f( )	Probability density function of the quantity in parenthesis
F( )	Cumulative distribution of the quantity in parenthesis
g	Acceleration of gravity
h	Height of slope
h_o	Vertical coordinate of the center of the failure surface (random variable)
k	Constant
ℓ	Length
L	Length of failure surface
L_d	Length of initial discontinuity
m	Earthquake magnitude
m_o	Lower limit of earthquake magnitude
m_1	Upper limit of earthquake magnitude
n	Number of earthquakes
n_m	Number of earthquakes with a magnitude larger than m
N	Normal component of force along failure surface
p	Probability

English Characters (continued)

p_a	Probability of earthquake acceleration being greater than a
p_f	Probability of failure
P[ ]	Probability of the event in brackets
r	Radial distance from center to point on failure surface
r_o	Initial radius of failure surface
r_u	Pore pressure parameter
R	Total available strength along failure surface (random variable)
S	Total driving force along failure surface (random variable)
$t(=\tan\phi)$	Tangent of the ϕ-parameter of soil strength (random variable)
T	Tangential component of force along failure surface
u	Pore water pressure
w	Height of water table above failure surface
W	Weight of soil material
x,y,z	Space variables

Greek Characters

α	Angle between earthquake acceleration vector and the horizontal direction
β	Angle of soil slope
β	Regional seismic parameter for the log-linear frequency-magnitude relation
γ_m	Moist unit weight of soil above water table
γ'_m	Submerged unit weight of soil
γ_s	Saturated unit weight of soil
δ	Angle between the tangent to failure surface and horizontal direction

Greek Characters (continued)

ε	Log-normally distributed error term appearing in the attenuation relationship
θ	Angle between radius r and initial radius r_o
θ_o	Angle between initial radius r_o and vertical direction (random variable)
θ_I	Angle between initial radius r_o and radius to lowest point I of the failure surface
θ_H	Angle between initial radius r_o and radius corresponding to the end point H of failure surface
λ	Mean earthquake occurrence rate
ϕ	Strength parameter of soil (random variable)

ABSTRACT

The present work provides a model for probabilistic stability analysis of earth slopes under earthquake loading. Significant uncertainties associated with conventional pseudo-static methods of seismic stability analysis are recognized and probabilistic tools are introduced for their description and amelioration. In particular, the proposed method of analysis accounts for (a) the variability of material strength parameters, (b) the uncertainty in the exact location of potential failure surfaces, and (c) the uncertainty in the value of the maximum slope acceleration during an earthquake.

The soil material comprising the slope is assumed to be probabilistically homogeneous with strength parameters (c and $t=\tan\phi$) being identically distributed random variables with given statistical values. Potential failure surfaces are considered to have an exponential shape (log-spiral), defined with the aid of three random variables (two geometric parameters and the frictional strength parameter).

The safety of the slope is measured in terms of its probability of failure (p_f) rather than the customary factor of safety. The numerical values of p_f are obtained through a Monte Carlo simulation of failure.

The seismic load is introduced into the analysis through the maximum horizontal acceleration (a_{max}) experienced by the slope during an earthquake. This is assumed to be a random variable, the probability distribution of which is found to depend on the earthquake magnitude, the type of earthquake source considered (i.e., point, line, or area source), the distance

between the source and the site and a number of regional parameters. In addition, for the purposes of this study, it is assumed that the slope is rigid, and therefore, the maximum acceleration of the slope mass is equal to that of the ground.

Two different attenuation relationships are employed to determine the maximum horizontal ground acceleration and the corresponding results are compared and discussed.

1. PROBABILISTIC SEISMIC STABILITY ANALYSIS

1.1 Introduction

Soil slopes, whether naturally formed or man-made (in the form of earth dams, cuts, embankments, etc.), are among the most frequently encountered geotechnical structures. Although much experience has already accumulated about their design and performance, geotechnical engineers still face considerable uncertainties when they analyze their stability. These uncertainties reflect the slope's loading conditions, the ground water conditions, the material parameters, the location and shape of the potential failure surface, the particular method used in the analysis, etc. The possibility of an earthquake renders such analyses even more complicated.

Conventionally, the safety of soil slopes is measured in terms of a "factor of safety (F_s)". In general, this factor is arbitrary in scale since it merely reflects whether a structure is safe ($F_s \geq 1$), or unsafe ($F_s < 1$). A factor of safety of two, for example, does not necessarily imply that the slope is twice as safe as one with a factor of safety of one. It simply states that the former is safer than the latter. The confidence with which one should view the factor of safety is also open to question. The literature is filled with reports of structures which have failed with factors of safety greater than one, and others, which have shown a remarkable success with factors as low as 0.6 [23].

To overcome the shortcomings associated with the conventional analysis, geotechnical engineers have suggested the use of more rational approaches to design, based on probability theory and reliability analysis [e.g., 20,21, 41, 51]. In particular, probabilistic slope stability analysis has been pursued by Wu and Kraft [50], Matsuo and Kuroda [28], Catalan and Cornell [11], Vanmarcke [44] and Alonso [1], among others.

A probabilistic formulation of the slope stability problem is based on the recognition that both the available resistance (R) and the driving load (S) along a potential failure surface are random variables. The difference between R and S is also a random variable often called the safety margin SM (i.e., SM = R - S). Failure of the slope occurs when its safety margin SM receives a negative value; i.e.,

$$\text{"Failure"} = [SM = R - S < 0]$$

The probability of the occurrence of this event is equal to the probability of failure p_f of the slope. Thus,

$$p_f = P[\text{Failure}] = P[SM < 0] \tag{1-1}$$

where P[ ] denotes the probability of the occurrence of the event in brackets.

The complement of the probability of failure is called the reliability $\bar{R}$ of the slope. Hence,

$$\bar{R} = 1 - p_f \tag{1-2}$$

If $f_R(R)$ and $f_S(S)$ represent the probability density functions of the resistance R and loading S, respectively, the expression for the probability of failure becomes [20]

$$p_f = \int_{-\infty}^{\infty} F_R(S)\, f_S(S)\, dS \tag{1-3}$$

where $F_R(\ )$ is the cumulative distribution of the resistance R.

In the case where the density functions of both the resistance and the loading receive simple analytical expressions (e.g., uniform, exponential, normal, lognormal, etc.), the probability of failure may be determined by performing the integration indicated in Equation (1-3). In Table 1 are given the analytical expressions for the probability of failure p_f for some frequently employed empirical distributions for the capacity of a structure C (its resistance) and the demand D (the applied loading) [4]. If, on the other hand, the expressions for the density functions for the resistance and loading are complicated (as is often the case in actual geotechnical situations), the integration indicated in Equation (1-3) is not easy to accomplish analytically. In this case, solutions must be obtained numerically or by using some simulation technique.

TABLE 1. PROBABILITY OF FAILURE FOR SOME EMPIRICAL MODELS (after [4])

DISTRIBUTION OF C AND D	$f_C(c)$	$f_D(D)$	P_f
uniform	$\frac{1}{C_{max} - C_{min}}$	$\frac{1}{D_{max} - D_{min}}$	$\frac{1}{2}\frac{D_{max} - 2C_{min} + D_{min}}{C_{max} - C_{min}}$
exponential	$a_C \exp(-a_C C)$	$a_D \exp(-a_D D)$	$\frac{a_D}{a_C + a_D}$
normal	$\frac{1}{S_C\sqrt{2\pi}} \exp[-\frac{1}{2}(\frac{C-\bar{C}}{S_C})^2]$	$\frac{1}{S_D\sqrt{2\pi}} \exp[-\frac{1}{2}(\frac{D-\bar{D}}{S_D})^2]$	$\frac{1}{2}\,\mathrm{erf}[\frac{\bar{C}-\bar{D}}{\sqrt{(S_C^2 + S_D^2)}}]$*
log-normal	$\frac{1}{CS_{\ell n}\sqrt{2\pi}} \exp[-\frac{1}{2}(\frac{\ell nC-\overline{\ell nC}}{S_{\ell nC}})^2]$	$\frac{1}{DS_{\ell nD}\sqrt{2\pi}} \exp[-\frac{1}{2}(\frac{\ell nD-\overline{\ell nD}}{S_{\ell nD}})^2]$	$\frac{1}{2}\,\mathrm{erf}[\ell n(\frac{\bar{C}}{\bar{D}}\sqrt{\frac{1+V_D^2}{1+V_C^2}})/\sqrt{\ell n(1+V_C^2)(1+V_D^2)}]$*
Rayleigh	$a_C C\exp(-a_C C^2/2)$	$a_D D\exp(-a_D D^2/2)$	$-\frac{4a_C(a_C+2a_D)}{a_D(a_C + a_D)}$
gamma	$\frac{\lambda^n C^{n-1} e^{-\lambda C}}{\Gamma(n)}$	$\frac{\mu^m D^{m-1} e^{-\mu D}}{\Gamma(m)}$	$1-\frac{\Gamma(m+n)}{\Gamma(m)\Gamma(n)} B_{\mu/(\mu+\lambda)}(m,n)$*
beta	$\lambda_C(C-C_{min})^{\alpha_C-1}(C_{max}-C)^{\beta_C-1}$	$\lambda_D(D-D_{min})^{\alpha_D-1}(D_{max}-D)^{\beta_D-1}$	$\lambda_D\int_{D_{min}}^{D_{max}}\frac{B_u(\alpha_C,\beta_C)}{B(\alpha_C,\beta_C)}(D-D_{min})^{\alpha_D-1}(D_{max}-D)^{\beta_D-1}dD$*
Weibull	$\frac{\beta_C}{\theta_C}(\frac{C-C_{min}}{\theta_C})^{\beta_C-1}\exp[-(\frac{C-C_{min}}{\theta_C})^{\beta_C}]$	$\frac{\beta_D}{\theta_D}(\frac{D-D_{min}}{\theta_D})^{\beta_D-1}\exp[-(\frac{D-D_{min}}{\theta_D})^{\beta_D}]$	$\int_0^\infty e^{-y}\exp[-[\frac{\theta_C}{\theta_D}y^{1/\beta_C} + (\frac{C_{min}-D_{min}}{\theta_D})]^{\beta_D}]dy$

*Note: erf [ ] = error function
B ( ) = beta function
B_u ( ) = incomplete beta function, $u = (D-C_{min})/(C_{max}-C_{min})$

1.2 Description of Failure Surfaces

The shape of the surface along which soil slopes fail is most frequently assumed to be of a planar or circular cylindrical form. Different shapes, however, have also been employed in the past. Collin [14] introduced cycloidal surfaces to analyze the stability of soil slopes while Rendulic [33] and Fröhlich [18] assumed that slopes slide along paths having the shape of a logarithmic spiral. The same mode of failure was later employed by other investigators [e.g., 17]. Furthermore, the sliding block type of failure has also been considered [10,30], especially when well defined zones exist within the soil profile. Finally, irregular shapes have been introduced by assuming failure surfaces to be composed of line segments with inclinations to the horizontal following a Fibonacci sequence [10].

In a stochastic description of the development and propagation of failure surfaces inside slopes composed of particulate materials, it was found [6] that the most probable failure path followed an exponential law. More recently, a generalized limiting equilibrium method was applied by Baker et al [8] to the evaluation of the stability of soil slopes using the calculus of variations. In this formulation of the problem, the shape of the failure surface and the distribution of the normal stress along this surface were left as variables to be determined by the mathematical (as opposed to trial and error) minimization of the factor of safety. It was subsequently concluded that the most critical failure surface had the form of a logarithmic spiral.

In the present study, it is assumed that the failure surface, created interior to a soil slope during an earthquake, has an exponential shape (log spiral) expressed in the form (Figure 1)

$$r = r_o \exp(-\theta t) \tag{1-4}$$

where r = the radius of the spiral,

r_o = the initial radius (value of r for $\theta = 0$),

θ = the angle between r and r_o, and

t = $\tan\phi$, where ϕ = soil strength parameter.

The location in the interior of the slope mass of a potential failure surface, as given by Equation (1-4) and illustrated in Figure 1, depends on the following three factors:

(1) the position along the slope boundary of the initiation point (point A),

(2) the location of the center of the log spiral (point O), and

(3) the numerical value of the ϕ-parameter of soil strength.

In general, the point of initiation of the failure surface is not known in advance. Studies on the development and propagation of failure surfaces in elastic slopes have indicated that the most likely point for the initiating of failure is the toe of the slope [34]. Failure surfaces initiation at specified points on the ground surface (along the base of the slope) have also been used [10]. In the present study, the assumption is made that failure surfaces pass through the toe of the slope.

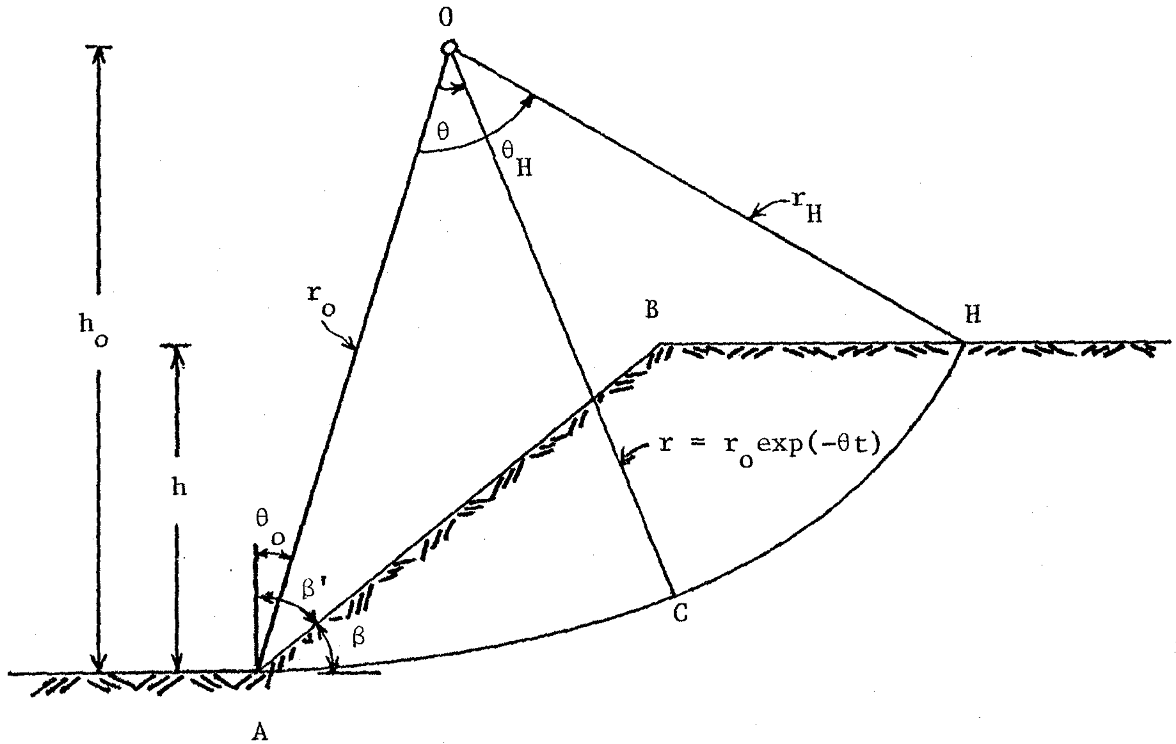

FIGURE 1. SHAPE OF FAILURE SURFACE

The center of the log spiral may be expressed in polar coordinates by means of two variables, h_o and θ_o (Figure 1). Introducing $h_o = r_o \cos\theta_o$ into Equation (1-4), the latter receives the form

$$r = \frac{h_o}{\cos\theta_o} \exp(-\theta t) \tag{1-5}$$

The uncertainty around the exact location of the center 0 of the log spiral can be accounted by considering its polar coordinates h_o and θ_o to be random variables receiving values within specified intervals; i.e.,

$$h_{o,min} \leq h_o \leq h_{o,max}$$

$$\theta_{o,min} \leq \theta_o \leq \theta_{o,max}$$

where $h_{o,min}$, $\theta_{o,min}$ and $h_{o,max}$ and $\theta_{o,max}$ are the minimum and maximum values that can be received by h_o and θ_o, respectively. Taking advantage of previous experience with log spiral failure surfaces [18,33], the limiting values of h_o and θ_o may be taken empirically to be $h_{o,min} = 0$, $h_{o,max} = 3h$ and $\theta_{o,min} = \beta'-\pi/3$, $\theta_{o,max} = \beta'$, where $\beta' = \pi/2-\beta$, and h and β are the height and angle of the slope, respectively. Furthermore, random variables h_o and θ_o are assumed to follow the general beta distribution expressed in the form [20]

$$f(x) = \lambda_x (x-x_{min})^{\alpha_x} (x_{max}-x)^{\beta_x}, \quad x_{min} < x < x_{max} \tag{1-6}$$

where x represents h_o or θ_o,

x_{min}, x_{max} are the minimum and maximum values of x respectively,

α_x, β_x are the parameters of the beta distribution,

$$\lambda_x = \frac{\Gamma(\alpha_x+\beta_x+2)}{\Gamma(\alpha_x+1)\Gamma(\beta_x+1)} \cdot \frac{1}{(x_{max} - x_{min})^{1+\alpha_x+\beta_x}} \text{, and}$$

$\Gamma(\ )$ is the gamma function.

Parameters α_x and β_x of the beta distribution can be obtained in terms of the statistical values of x as follows [20]:

$$\alpha_x = \frac{\tilde{x}^2}{\tilde{V}}(1 - \tilde{x}) - (1 + \tilde{x})$$

$$\beta_x = \frac{\alpha_x + 1}{\tilde{x}} - (\alpha_x + 2)$$

where $\tilde{x} = (\bar{x} - x_{min})/(x_{max} - x_{min})$, and

$$\tilde{V} = \sigma_x^2/(x_{max} - x_{min})^2$$

In the subsequent applications of Equation (1-6), it will be also assumed that h_o and θ_o are symmetric around their mean values (i.e., $\alpha_x = \beta_x$).

According to the procedure presented above, for a fixed value of the strength parameter t (=tanϕ), the locations of the failure surface depend only on the values of the two geometric parameters h_o and θ_o. As an example, in Figure 2 are shown failure surfaces corresponding to characteristic values of h_o and θ_o. The slope considered has a height $h = 30$ ft and angle $\beta = 30°$, while the t parameter is taken equal to $t = 0.58$ ($\phi = 30°$).

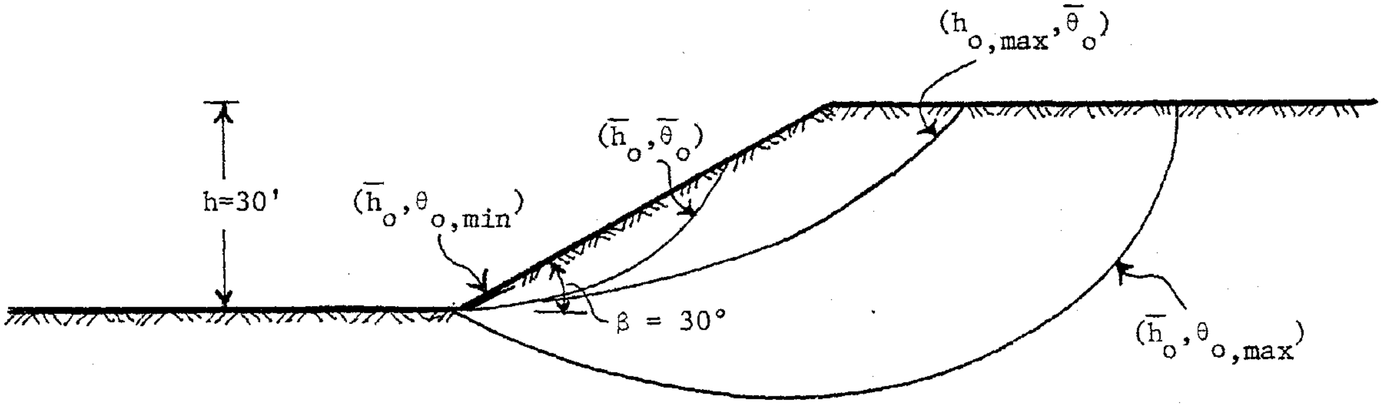

FIGURE 2. FAILURE SURFACES FOR CHARACTERISTIC VALUES OF THE CENTER COORDINATES h_o and θ_o.

1.3 Mean Failure Surface

Let r, h_o, θ_o and t, appearing in Equation (1-5), be denoted by y, x_1, x_2 and x_3, respectively. Equation (1-5) may then be rewritten as

$$y = y\ (x_1,x_2,x_3) = \frac{x_1}{\cos x_2} \exp(-\theta x_3) \tag{1-7}$$

in which x_1, x_2 and x_3 are independent random variables.

If the mean values and standard deviations of random variables x_i, i = 1,2,3, are known, then an approximate expression for the mean value $\bar{y}$ of function y can be obtained by using a method developed by Rosenblueth [35]. To illustrate this method, consider first that y is a function of a single variable x, the skewness coefficient of which is unknown or nil. Rosenblueth showed that $\bar{y}$ may be obtained as the average of two point estimates of y(x): one for $x = \bar{x} + \sigma_x$ and, another, for $x = \bar{x} - \sigma_x$, where $\bar{x}$ and σ_x are the mean value and standard deviation of x, respectively. Thus, in the case of a function of one variable, $\bar{y}$ is approximately equal to

$$\bar{y} \cong \frac{1}{2}\sum_{i=1}^{2} y_i(\bar{x} \pm \sigma_x) = \frac{1}{2}[y(\bar{x}+\sigma_x) + y(\bar{x}-\sigma_x)]$$

Similarly, the mean value $\bar{y}$ of the function given by Equation (1-7) is equal to

$$\bar{y} \cong \frac{1}{8}\sum_{i=1}^{8} y_i(\bar{x}_1 \pm \sigma_{x_1},\ \bar{x}_2 \pm \sigma_{x_2},\ \bar{x}_3 \pm \sigma_{x_3}) \tag{1-8}$$

where the eight point estimates of y correspond to the eight possible combinations of the values $x_i = \bar{x}_i \pm \sigma_{x_i}$, i = 1,2,3. That is, the first term in the summation on the RHS of Equation (1-8) is $y_1 = y(\bar{x}_1+\sigma_{x_1},\ \bar{x}_2+\sigma_{x_2},\ \bar{x}_3+\sigma_{x_3})$, the second term is $y_2 = y(\bar{x}_1+\sigma_{x_1},\ \bar{x}_2+\sigma_{x_2},\ \bar{x} - \sigma_{x_3})$, the third term is $y_3 = y(\bar{x}_1+\sigma_{x_1},\ \bar{x}_2-\sigma_{x_2},\ \bar{x}_3+\sigma_{x_3})$, and so on.

As an example, consider a slope of a height $h = 20$ ft. and angle $\beta = 45°$ (Figure 3). The material strength parameter $t(=\tan\phi)$ is assumed to have a mean value $\bar{t} = 0.58$ ($\bar{\phi} = 30°$) and a coefficient of variation $V_t = 15\%$. In Table 2 are listed the mean values $(\bar{x}_i)$, standard deviations (σ_{x_i}) and the points of evaluation $(\bar{x}_i \pm \sigma_{x_i})$ of the random variables x_i, $i = 1,2,3$. The center of the failure surface that corresponds to $(\bar{x}_1 + \sigma_{x_1}, \bar{x}_2 + \sigma_{x_2})$ is shown in Figure 3 as point 0_{++}. Similarly, points 0_{+-}, 0_{-+}, and 0_{--} have coordinates $(\bar{x}_1+\sigma_{x_1}, \bar{x}_2-\sigma_{x_2})$, $(\bar{x}_1-\sigma_{x_1}, \bar{x}_2+\sigma_{x_2})$ and $(\bar{x}_1-\sigma_{x_1}, \bar{x}_2-\sigma_{x_2})$, respectively. Two failure surfaces correspond to each center depending on the value of the strength parameter x_3: one, for $x_3 = \bar{x}_3 + \sigma_{x_3}$ and, another, for $x_3 = \bar{x}_3 - \sigma_{x_3}$. The mean failure surface (with its angle at 0), obtained using Equation (1-8), is shown in Figure 3.

If, on the other hand, in determining $\bar{y}$ the variations of x_1, x_2 and x_3 were neglected while their point estimates were taken to be equal to their mean values, the corresponding expression for $\bar{y}$ would be

$$\bar{y} \cong y(\bar{x}_1, \bar{x}_2, \bar{x}_3) \tag{1-8a}$$

Thus, for the case of the slope examined in the above example, $\bar{y}$ would be reduced to

$$\bar{y} \cong y(30, 15, 0.58) = 31.06 \exp(-0.58\theta)$$

This expression for $\bar{y}$ is also shown in Figure 3 from which it can be seen that $\bar{y}$ lies very close to the mean failure surface obtained using Equation (1-8).

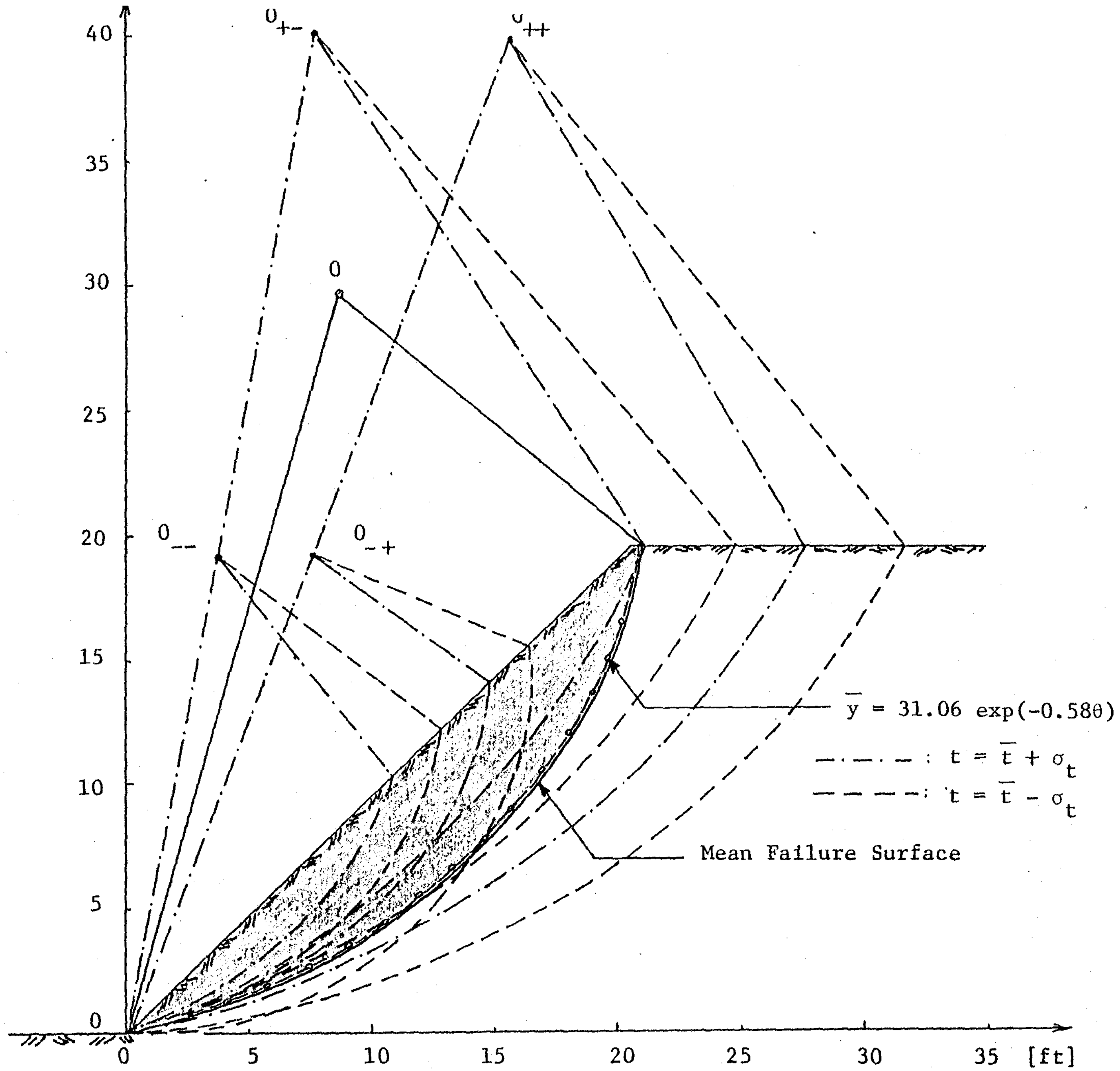

FIGURE 3. MEAN FAILURE SURFACE FOR ILLUSTRATIVE EXAMPLE

TABLE 2. STATISTICAL VALUES AND POINTS OF EVALUATION OF THE THREE RANDOM VARIABLES h_o, θ_o and t.

Random Variable x_i	Mean Value $\bar{x}_i$	Standard Deviation σ_{x_i}	Points	
			$\bar{x}_i+\sigma_{x_i}$	$\bar{x}_i-\sigma_{x_i}$
x_1 $(=h_o)$ (ft)	30	10.50	40.50	19.5
x_2 $(=\theta_o)$ (degrees)	15	5.25	20.25	9.75
x_3 $(=t)$	0.58	0.087	0.667	0.493

1.4 Resisting and Driving Forces Along Failure Surfaces

The static forces acting on a differential element along the failure surface are shown in Figure 4. The weight dW of a slice of width dx is equal to

$$dW = \gamma_m(z-w)\ dx + \gamma_s\ w\ dx \tag{1-9}$$

where γ_m = the total unit weight of the soil above the water table,

γ_s = the saturated unit weight,

z = the distance from the failure surface to the slope boundary, and

w = the distance from the failure surface to the water table.

The location of the water table is defined by the dimensionless parameter r_u expressed as [9]

$$r_u = \frac{u}{\gamma_m(z-w)+\gamma_s w} \tag{1-10}$$

where u is the pore water pressure at the failure surface (assumed hydrostatic), and z, w, γ_s and γ_m are defined in Equation (1-9). The distance w from the failure surface to the water table is found from Equation (1-10) as

$$w = \frac{u}{\gamma_w} = r_u \frac{\gamma_m}{\gamma_w + r_u(\gamma_m-\gamma_s)}\ z$$

where γ_w is the unit weight of the water.

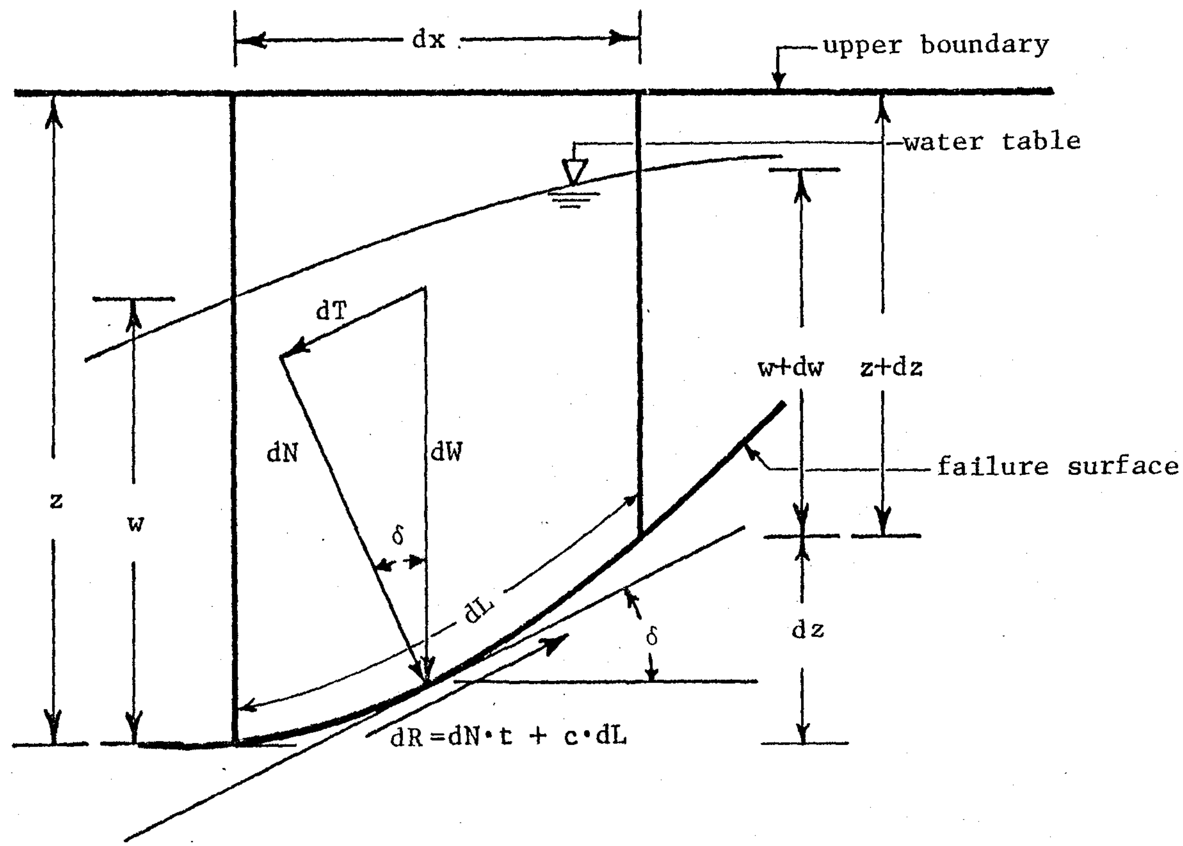

FIGURE 4. FORCES ON A DIFFERENTIAL ELEMENT ALONG THE FAILURE SURFACE

The normal and tangential (to the failure surface) components of the weight dW are denoted by dN_w and dT_w, respectively, and are equal to

$$\begin{aligned} dN_w &= dW \cos \delta \\ dT_w &= dW \sin \delta \end{aligned} \tag{1-11}$$

where δ (Figure 4) is the slope of the failure surface.

In the present study, the additional load on the slope due to an earthquake will be introduced in terms of the maximum value of the acceleration $\underline{a}$ at the site of the slope. Furthermore, it will be assumed that the magnitude of the vertical component (with an upward direction) of the maximum acceleration is equal to two-thirds of that of the horizontal component (with a direction away from the slope) [43]; and that both act on the slope mass simultaneously. Thus, the angle $\underline{\alpha}$ between the maximum acceleration $\underline{a}$ and the horizontal direction is equal to 33.7° ($\alpha = 33.7°$).

Because of the uncertainties involved in determining the maximum acceleration, the latter will be considered as a random variable the statistical characteristics of which will be examined in detail in Section 2 of this report.

The components of the earthquake loading along the normal and tangential direction of the failure surface are equal to

$$\begin{aligned} dN_{eq} &= dW \cdot a \cdot \sin[-(\alpha + \delta)] \\ dT_{eq} &= dW \quad a \quad \cos(\alpha + \delta) \end{aligned} \tag{1-12}$$

By combining Equations (1-11) and (1-12), the values are found of the total normal (dN) and tangential (dT) forces acting on the differential segment of the failure surface; i.e.,

$$
\begin{aligned}
dN &= dN_w + dN_{eq} \\
dT &= dT_w + dT_{eq}
\end{aligned}
\tag{1-13}
$$

If the resisting and driving forces along dL (Figure 4) are denoted by dR and dS, respectively, one has

$$
\begin{aligned}
dS &= dT \\
dR &= dN \cdot t + c \cdot dL
\end{aligned}
\tag{1-14}
$$

where c and t are the two strength parameters of the soil material.

The failure surface given by Equation (1-5), may be expressed in Cartesian coordinates as follows:

$$x = x(\theta) = r_o \sin\theta_o + r_o \exp(-\theta t)\sin(\theta-\theta_o)$$

$$y = y(\theta) = r_o \cos\theta_o - r_o \exp(-\theta t)\cos(\theta-\theta_o)$$

The length dL of a differential element along the failure surface is equal to

$$dL = \{[x'(\theta)]^2 + [y'(\theta)]^2\}^{1/2} d\theta \tag{1-15}$$

where $x'(\theta)$ and $y'(\theta)$ are the derivatives of $x(\theta)$ and $y(\theta)$ with respect to θ; i.e.,

$$
\begin{aligned}
x'(\theta) &= r_o \exp(-\theta t)[\cos(\theta-\theta_o) - t\sin(\theta-\theta_o)] \\
y'(\theta) &= r_o \exp(-\theta t)[+\sin(\theta-\theta_o) + t\cos(\theta-\theta_o)]
\end{aligned}
\tag{1-16}
$$

Equations (1-15) and (1-16) are combined to yield

$$dL = dL(h_o, \theta_o, t) = r_o \exp(-\theta t)(1 + t^2)^{1/2} \, d\theta \tag{1-17}$$

Consequently, the total length L of the failure surface is equal to

$$L = \int_o^L dL = \int_o^{\theta_H} r(1 + t^2)^{1/2} \, d\theta \tag{1-18}$$

where r is given by Equation (1-4), and θ_H is the upper limit of angle θ (Figure 1) and corresponds to the terminal point of the failure surface along the slope boundary. After the integration indicated by Equation (1-18) is performed, it is found that

$$L = \frac{h_o}{\cos\theta_o} (1 + \frac{1}{t^2})^{1/2} \, [\exp(-\theta_H t) + 1] \tag{1-19}$$

The total resisting and driving forces, R and S, respectively, can be found through an integration of Equations (1-14); i.e.,

$$R = \int_0^L dR$$

$$S = \int_0^L dS \tag{1-20}$$

The developments presented above were concerned with failure surfaces originating at the toe of the slope. It is possible, however, that a discontinuity (e.g., a relic slip surface) already existed in the interior of the soil mass. Since its length L_d can be of any size between 0 and L, the probability density function of L_d can be assumed uniform in the interval (0,L), where L is given by Equation (1-19). Along L_d the c-parameter of strength is zero while t is assumed constant and equal to its mean value $\bar{t}$. The option to account in this manner for a possible initial discontinuity is available in the computer program RASSUEL (see Section 1.6)[5].

The integration of Equations (1-14) requires consideration of the relative position along the failure surface of three characteristic points. These are shown in Figure 5 (as points I, C and S). There are six possible arrangements of the three points (Figure 6), if a failure surface terminates at the boundary behind the crest of the slope; and two arrangements, if the surface ends on the slope (i.e., in this case, there is no point C).

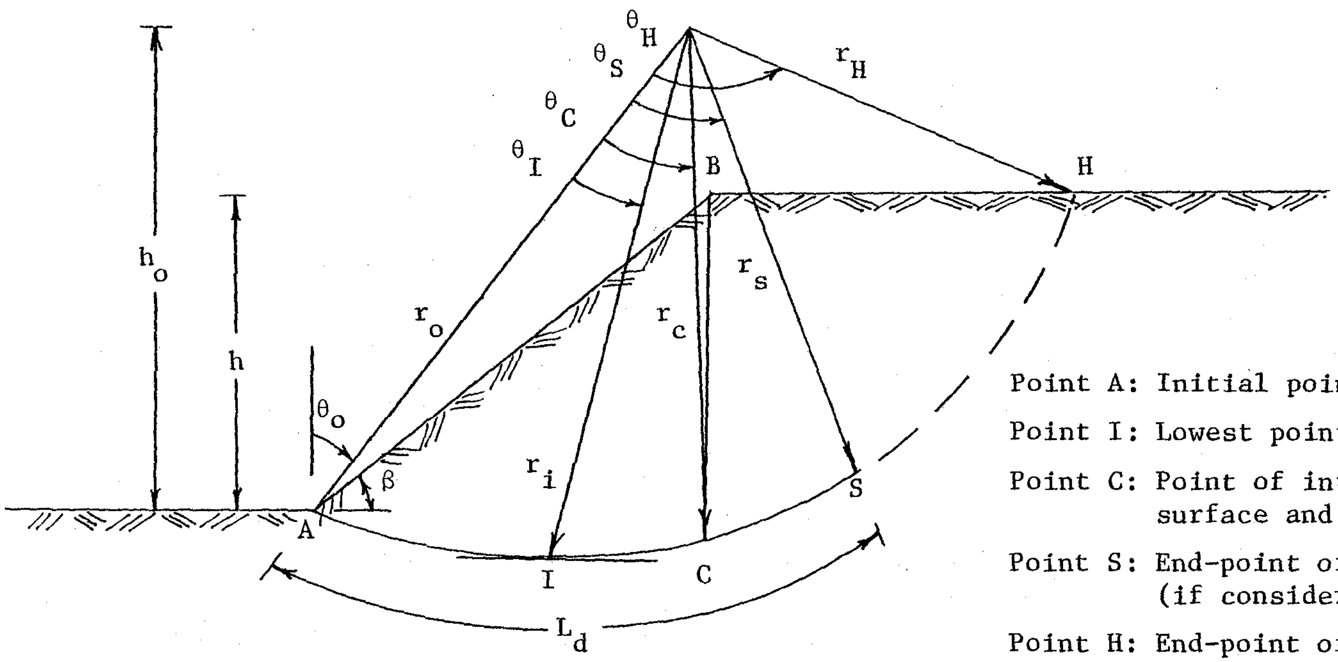

Point A: Initial point of failure surface.

Point I: Lowest point of failure surface.

Point C: Point of intersection between failure surface and the vertical through point B.

Point S: End-point of initial discontinuity (if considered)

Point H: End-point of failure surface.

FIGURE 5. SLOPE GEOMETRY WITH CHARACTERISTIC POINTS ALONG THE FAILURE SURFACE

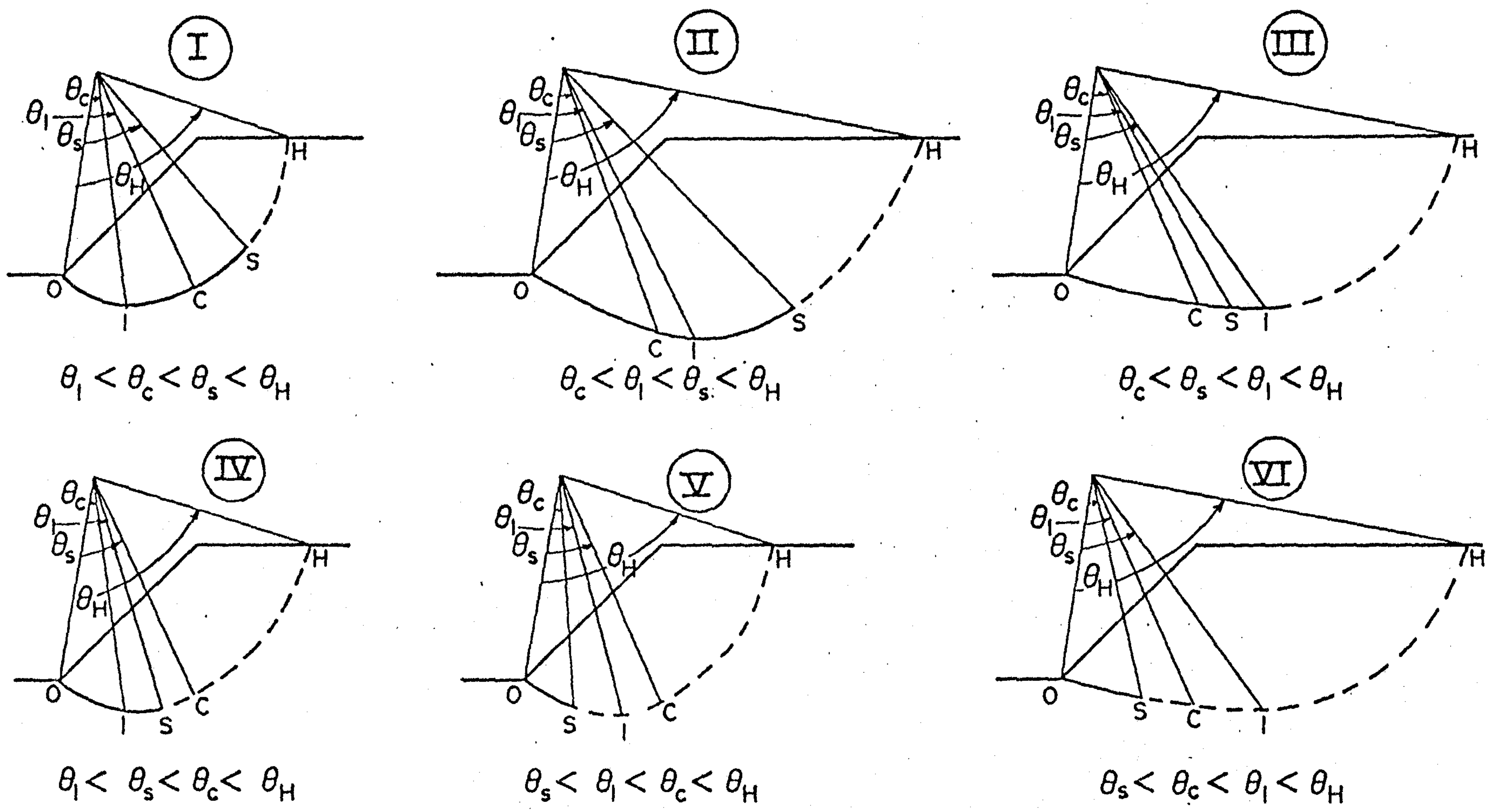

FIGURE 6. THE SIX POSSIBLE ARRANGEMENTS OF POINTS I, C AND S ALONG THE FAILURE SURFACE

1.5 Variability of Soil Strength Parameters

The uncertainty in the numerical values of soil strength may be attributed to the following three reasons:

(a) The limited information about actual subsurface conditions,

(b) Measurement or "engineering" errors, and

(c) The inherent variability of soil itself.

The last is by far the most important cause of uncertainty. On the basis of results obtained from a large number of tests on natural soils, it was found [25] that the inherent variability of soil was so great that the effects of test imprecision may be overwhelmed. Research studies have been recently undertaken with an objective to quantify this uncertainty and describe the spatial variation of soil strength and strength parameters [2,24,45].

To account for the variation in the numerical values of soil strength parameters, geotechnical engineers have considered them to be random variables and have proposed probabilistic models for their description. Thus, Lumb [27] found that the two strength parameters (c and t) followed a normal distribution. This conclusion was drawn from his study on a large amount of test data from soils of the area of Hong Kong (namely, a soft marine clay, a residual silty sand, an alluvial sandy clay and a residual clayey silt). Additional studies of frequency distributions of soil properties [i.e.,37,40,etc.] came to support Lumb's conclusion that strength parameters are normal-like variates.

In a more recent work, however, Lumb [26] found that the c-parameter of strength followed more closely a beta rather than a normal distribution, and that only its central portion could be approximated as a normal variate. The use of the beta distribution for modelling soil strength parameters was also suggested by Harr [20] who, recognizing the versatility of the beta model, recommended its use to obtain approximations for many geotechnical data sets whose measures must be positive and of a limited range (in contrast to normal variates that receive values between $-\infty$ and ∞).

In compliance with the above findings, the present study assumes that strength parameters c and t (=tanϕ) are random variables following the beta (or, Pearson's type I) distribution, given by Equation (1-6).

1.6 Probability of Failure

In Section 1.4, the resisting and driving forces along a potential failure surface of a soil slope have been expressed as integrals of functions containing a number of random variables (Equations 1-20). As it was stated in the Introduction, use of a numerical scheme is necessary in order to determine the probability of failure p_f of a structure if its load and resistance are not simple analytical functions (such as those appearing in Table 1). In this study, the numerical values of p_f are determined through a Monte Carlo [19,36] simulation of failure. A flow chart indicating the operations that led to the probability of failure is given in Figure 7.

The Monte Carlo simulation of failure involves (a) the generation of failure surfaces by selecting values of three random variables: two geometric parameters (h_o and θ_o) and strength parameter t (=tanϕ), and (b) the calculation of the total resistance R and driving force S (acting along the generate failure surface) by selecting values from two additional random variables: strength parameter c and slope's maximum horizontal acceleration a_{max}. If this procedure is repeated N times and the event "failure" (i.e., R < S) occurs M times, then the probability of failure p_f is close to the relative frequency M/N, provided that N is large enough [32]; i.e.,

$$p_f = \frac{M}{N}$$

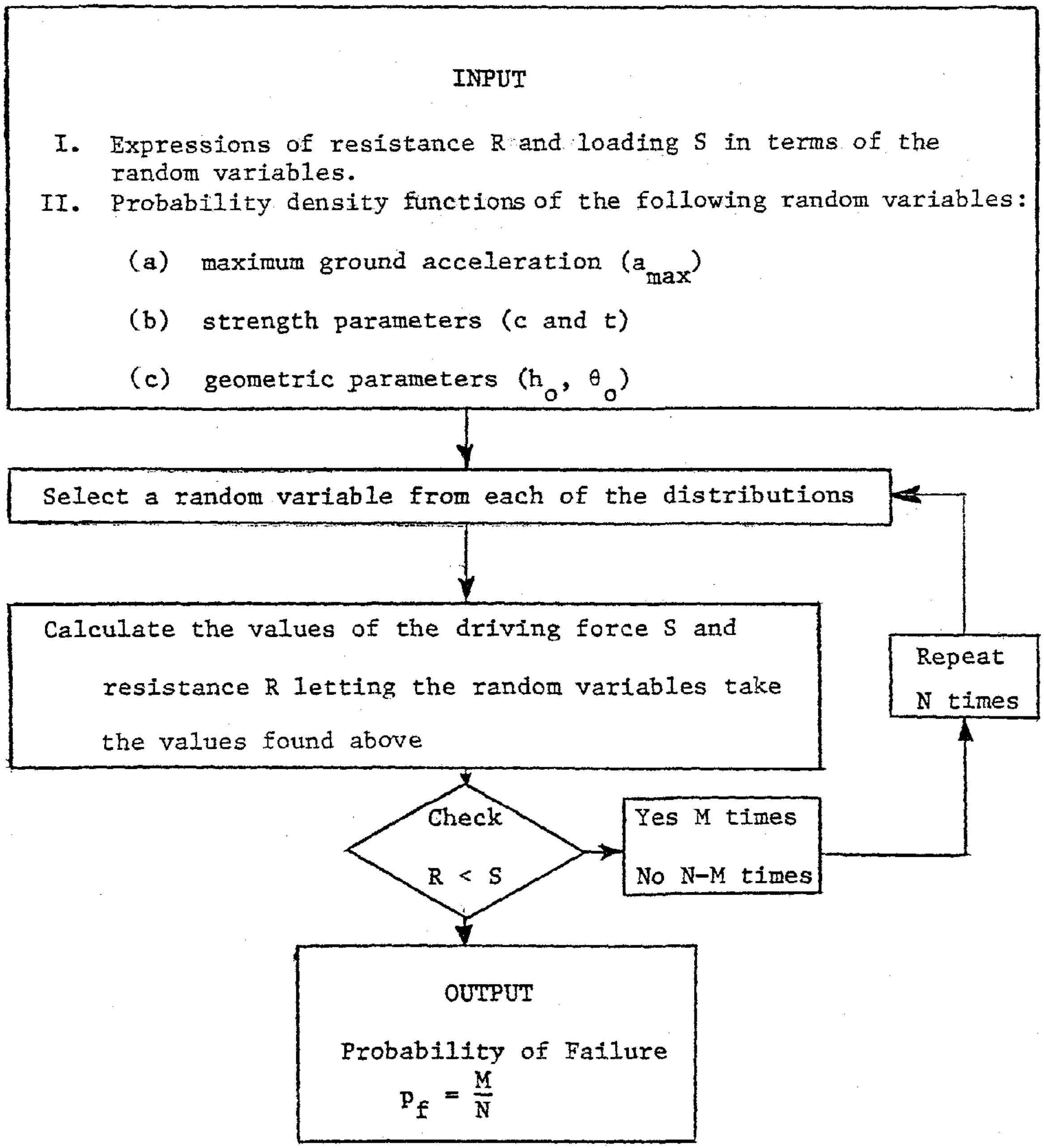

FIGURE 7. FLOW CHART OF THE OPERATIONS INVOLVED IN DETERMINING THE PROBABILITY OF FAILURE

The present probabilistic seismic stability analysis has been incorporated into a computer program called RASSUEL. A description of the program and its capabilities together with guidelines for its use is given in a separate report [5]. The flow chart for program RASSUEL is shown in Figure 8.

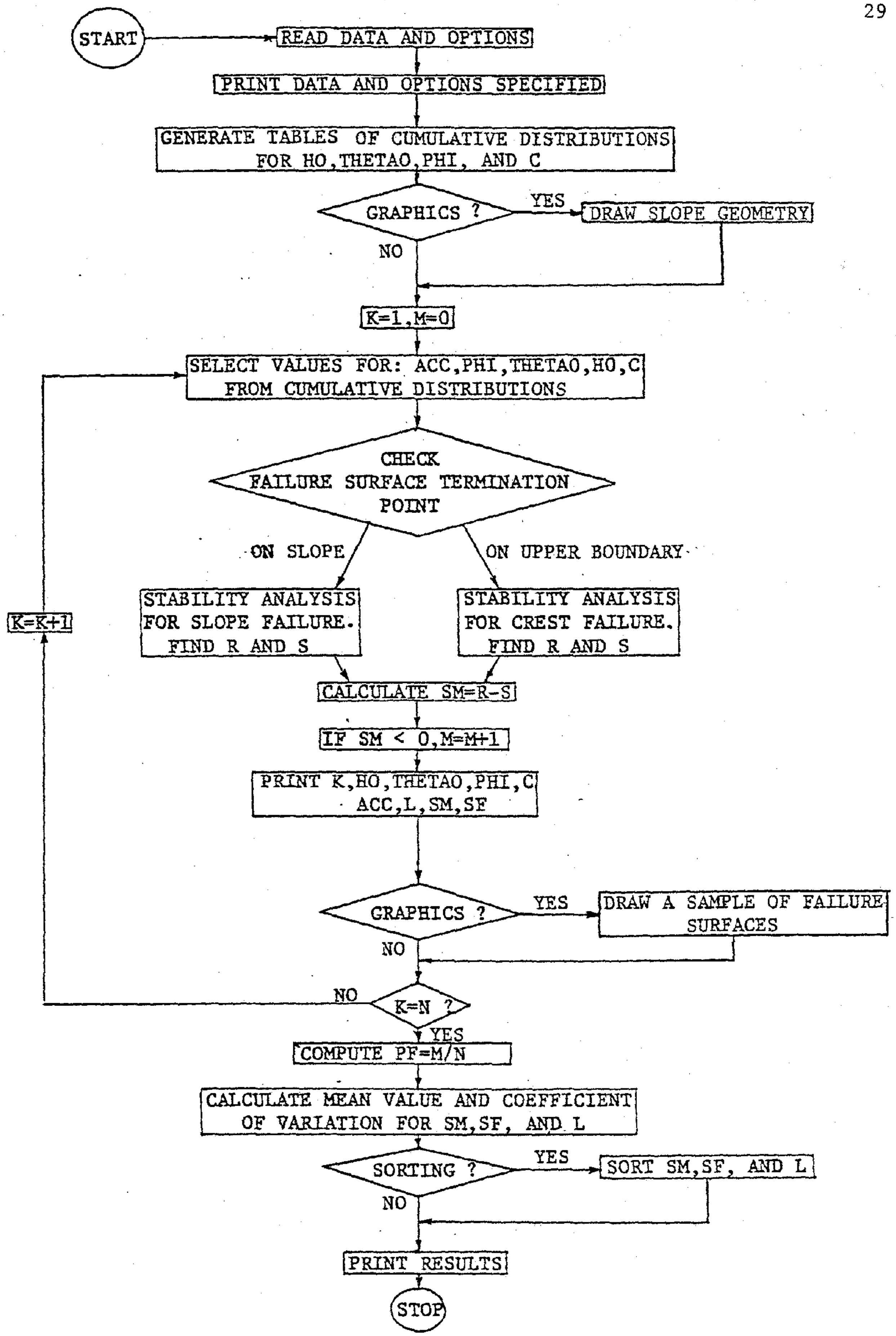

FIGURE 8. FLOW CHART FOR PROGRAM 'RASSUEL'

2. STATISTICAL DESCRIPTION OF SEISMIC PARAMETERS

2.1 Introduction

From an engineering point of view, one is interested in one or more parameters that reflect ground motion characteristics rather than in the details of an earthquake record. Examples of such parameters are the maximum value of the ground acceleration, velocity or displacement, the spectral ordinates, the duration of the earthquake, etc. In the model presented in the previous section, the effect of an earthquake on the stability of soil slopes was introduced through the maximum value of the horizontal acceleration (a_{max}) experienced at the site of the slope.

There are many factors which affect the numerical values of a_{max} and they may be divided into three categories [22]; namely, (a) source factors (e.g., location and dimension of source, stress conditions at the source, radiation pattern, etc.), (b) travel path (e.g., geometric spreading of waves, energy absorption, inhomogeneities of medium, etc.), and (c) local conditions (e.g., subsurface conditions, topographic variations, etc.). Although considerable research effort is underway aiming at an improved description of each significant factor, the available information is utilized in the current state-of-the-art through a limited number of representative parameters from each category. Thus, the earthquake <u>magnitude</u> is employed to represent the source factors, the <u>distance</u> between source and site of interest reflects the travel path and local conditions are accounted through a number of <u>regional parameters</u>. In addition, the maximum acceleration of the slope mass is assumed to be identical to that of the ground (rigid body assumption).

Many relationships have been proposed over the years to provide the maximum horizontal ground acceleration (a_{max}) as a function of the earthquake magnitude (m), the distance (R) between source and site, and the regional parameters. Idriss [22], in his presentation of the state-of-the-art of ground motions, made reference to thirty-two such relationships that cover the period between 1956 and 1978. Predicted values of a_{max} are different for different relationships; and this disagreement in the results is often quite large, especially for sites close to the earthquake source.

In view of the inherent uncertainties in available attenuation relationships, any prediction for the maximum ground acceleration must be based on a statistical formulation of the problem. Thus, in the present study, a_{max} will be considered as a random variable and its frequency and cumulative distributions will be derived. The dependence of the latter on regional and other parameters will be also investigated. Finally, as one of the objectives of this study is to provide a stability analysis for soil slopes located in the seismic environment of the State of New York, regional parameters will receive values pertinent to this part of the country.

2.2 Earthquake Magnitude

The empirical formula most commonly employed to yield the number of earthquakes n_m exceeding a certain magnitude m is Richter's log-linear relationship [16] expressed in the form

$$\log n_m = a - bm \qquad (2\text{-}1)$$

where a and b are regional constants.

The natural logarithm of n_m can be obtained from Equation (2-1) as

$$\ln n_m = (\ln 10)(\log n_m) = (\ln 10)(a-bm)$$

from which one has than n_m is equal to

$$n_m = \exp[(\ln 10)(a-bm)] = \exp(a\cdot\ln 10)\exp(-bm\cdot\ln 10)$$

or,

$$n_m = 10^a \exp(-\beta m) \qquad (2\text{-}2)$$

where $\beta = b \ln 10$.

For Equation (2-2) to gain engineering significance, lower and upper limits for magnitude m have to be imposed. Thus, if m_o and m_1 denote the lower and upper limits of m, respectively, Equation (2-2) becomes

$$\log n_m = a - b(m-m_o) \ , \qquad m_o \leq m \leq m_1 \qquad (2\text{-}3)$$

From Equation (2-2), one has that the expected number of earthquakes (n_{m_o}) with magnitude greater than the assumed lower bound (m_o) is equal to

$$n_{m_o} = 10^a \exp(-\beta m_o) \tag{2-4}$$

The ratio of n_m over n_{m_o} signifies the probability with which the earthquake magnitude M is greater than m [42]; i.e.,

$$P[M > m] = \frac{n_m}{n_{m_o}} = \frac{10^a \exp(-\beta m)}{10^a \exp(-\beta m_o)} = \exp[-\beta(m-m_o)], \quad m_o \leq m \tag{2-5}$$

The cumulative density function F(m) of the earthquake magnitude m is equal to

$$F(m) = P[M \leq m] = 1 - P[M > m]$$

Introducing Equation (2-5) into the above expression, it is found that

$$F(m) = 1 - \exp[-\beta(m-m_o)] \tag{2-6}$$

A normalizing factor is required so that F(m) becomes unity when m receives its maximum value m_1. If this factor is denoted by k, from Equation (2-6) one has

$$F(m_1) = k\{1 - \exp[-\beta(m_1-m_o)]\} = 1$$

or,

$$k = \{1 - \exp[-\beta(m_1-m_o)]\}^{-1} \tag{2-7}$$

Thus, F(m) may be written as

$$F(m) = \begin{cases} 0 & m < m_o \\ k\{1-\exp[-\beta(m-m_o)]\} , & m_o \leq m \leq m_1 \\ 1 & m_1 < m \end{cases} \tag{2-8}$$

where k is given in Equation (2-7).

The probability density function f(m) of the magnitude m can be found by forming the derivative of Equation (2-8) with respect to m. Thus, one has

$$f(m) = \begin{cases} 0 & m < m_o \\ \beta k \exp[-\beta(m-m_o)], & m_o \leq m \leq m_1 \\ 0 & m_1 \leq m \end{cases} \tag{2-9}$$

where k is given in Equation (2-7).

In the case of New York State, the lower and upper limits of the magnitude m have been found [31] to be equal to 2.0 and 6.3, respectively. For the Northeastern United States, the values of the β parameter varies between 1.35 and 1.54 [31]. In Table 3 are given the values of the β parameter for various seismic regions of the United States, while the world-wide range of values for β is between 1.61 and 2.88 [46].

The mean value and variance of the earthquake magnitude m are given by the following expressions:

$$\begin{aligned} \overline{m} &= \int_{-\infty}^{\infty} mf(m)\ dm \\ \mathrm{Var}(m) &= \int_{-\infty}^{\infty} (m-\overline{m})^2 f(m)dm \end{aligned} \tag{2-10}$$

where f(m) is the probability density function of m, given by Equation

TABLE 3. VALUES OF β-PARAMETER FOR VARIOUS SEISMIC REGIONS (after [46])

SEISMIC REGION	β	COMMENTS
Southern New England	2.19($\pm$0.12)	1800-1959; 135 events
New Jersey	2.17	
Central Mississippi River Valley	2.00($\pm$0.25)	1833-1972; 250,000 km^2
North and Central America	2.26	1963-1968
Southern California	1.94	1934-1963; 10,126 events 296,000 km^2
California	2.07	

(2-9). Substituting the latter into Equations (2-10) and performing the indicated integrations, it is found that

$$\bar{m} = k[m_o + \frac{1}{\beta} - (m_1 + \frac{1}{\beta}) \exp[-\beta(m_1 - m_o)]\}$$
$$\mathrm{Var}(m) = k\{m_o^2 - m_1^2 \exp[-\beta(m_1 - m_o)]\} + \frac{2\bar{m}}{\beta} - \bar{m}^2 \qquad (2\text{-}11)$$

In Figures 9 and 10 are shown the probability density function and cumulative distribution of m, respectively, for a value of the β-parameter equal to 1.35, 1.5, and 2.5.

In Appendix A are given the expressions for the probability density function and cumulative distribution of the earthquake magnitude for the case of a log-quadratic frequency-magnitude relationship. Such a relationship appears to best represent available seismic data for New York State and it is studied in detail in the third report of this series, RPI Report No. CE-78-7.

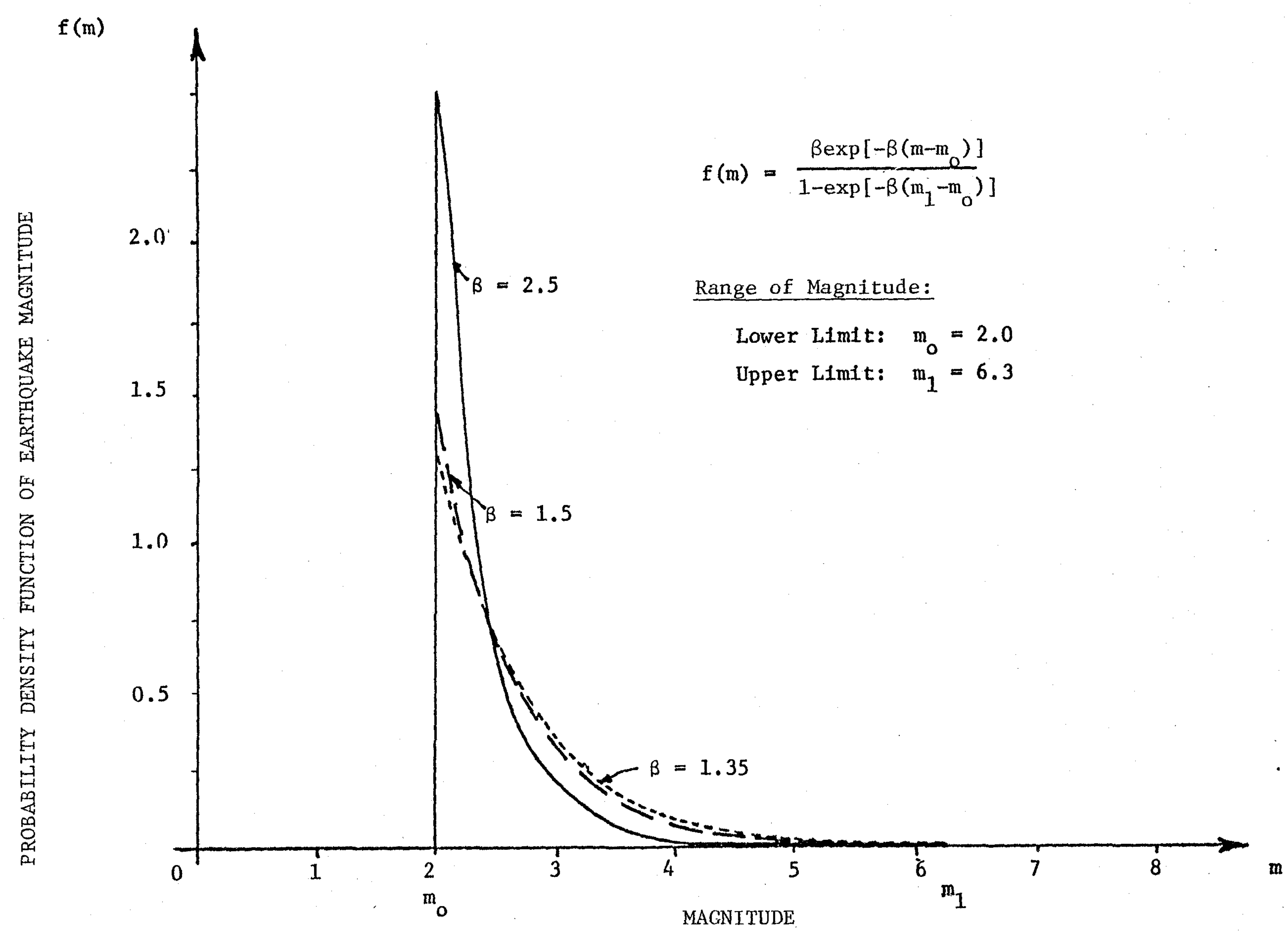

FIGURE 9. PROBABILITY DENSITY FUNCTION OF EARTHQUAKE MAGNITUDE

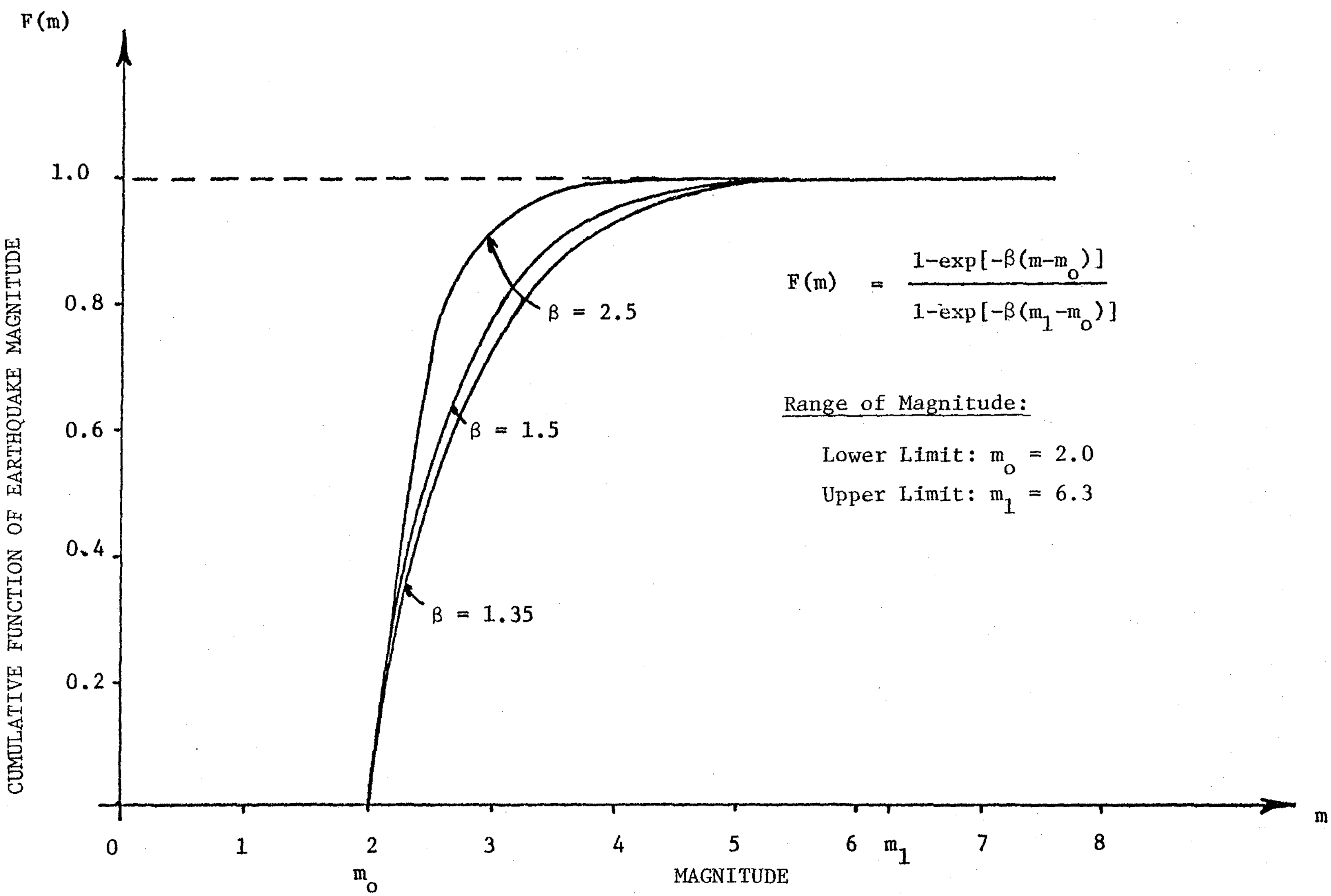

FIGURE 10. CUMULATIVE DISTRIBUTION OF EARTHQUAKE MAGNITUDE

2.3 Maximum Horizontal Ground Acceleration

The most frequently used attenuation relationships are expressed in the following form [16]:

$$a_{max} = b_1 \, e^{b_2 m} \, (R + b_4)^{-b_3} \tag{2-12}$$

where a_{max} is the maximum acceleration (in cm/sec), m is the earthquake magnitude, R is the distance between source and site (in km) and b_1, b_2, b_3 and b_4 are regional parameters. Values that have been proposed for these parameters are listed in Table 4.

Comparisons made between observed and computed values of ground motion parameters have indicated that their ratio follows closely a log-normally* distributed random variable. Denoting the latter by ε and introducing it into Equation (2-12), one has

$$a_{max} = b_1 \, e^{b_2 m} \, (R + b_4)^{-b_3} \, \varepsilon \tag{2-13}$$

The logarithm of ε has been found to have a mean value equal to zero ($\overline{\ln\varepsilon}=0$) and a standard deviation ($\sigma_{\ln\varepsilon}$) between 0.5 and 1.0 [29,31]

In general, three types of earthquake sources can be distinguished, namely, (a) a point source, (b) a line (or, fault) source, and (c) an area source. These are shown schematically in Figure 11.

A point source represents the fundamental case in seismic risk analysis. A line source is used for the seismic description of a region where a fault has been clearly identified. When this is not the case,

*A variable is log-normally distributed, if its natural logarithm is normally distributed.

TABLE 4. VALUES OF THE COEFFICIENTS OF THE ATTENUATION RELATIONSHIP

COEFFICIENT				
b_1	b_2	b_3	b_4	Reference
1960	0.8	2.0	0.0	50
1260	0.8	2.0	0.0	31,42
1350	0.58	1.52	0.0	31,42
*1100	0.5	1.32	25.0	31,42
1230	0.8	2.0	0.0	31
2000	0.8	2.0	0.0	31
*1.183	1.15	1.0	0.0	16,31
1200	0.8	2.0	0.0	29

*Values suggested for the Northeast United States

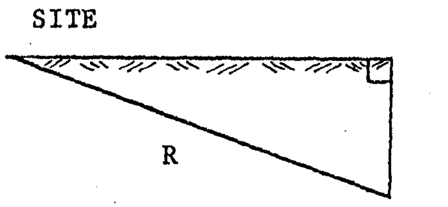

(a) Point Source (cross section)

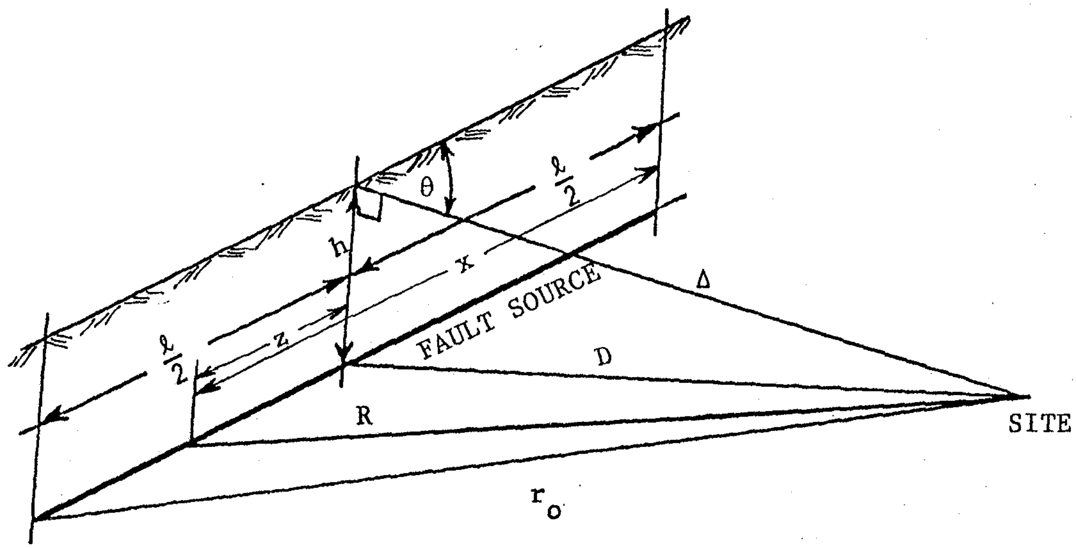

(b) Line Source (perspective)

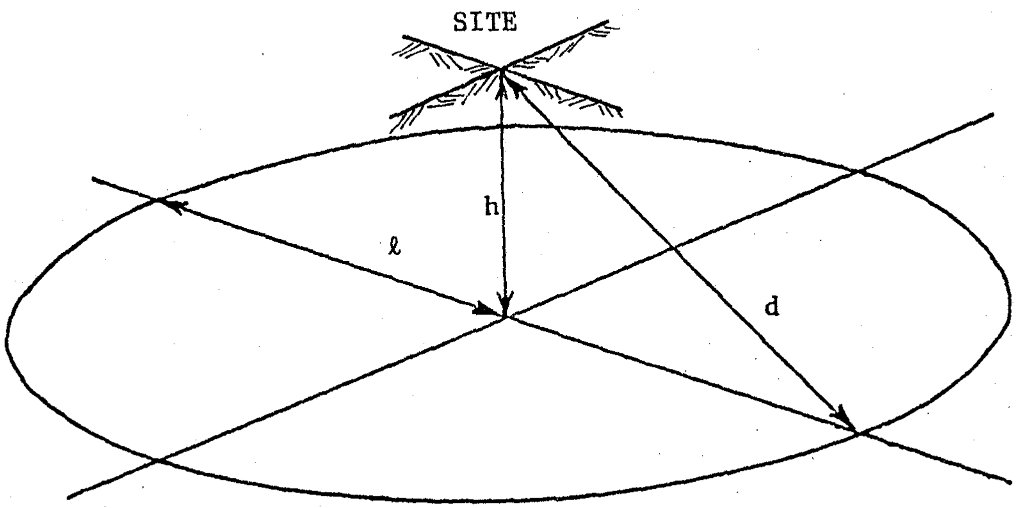

(c) Area Source (perspective)

FIGURE 11. SCHEMATIC REPRESENTATION OF THE THREE POSSIBLE EARTHQUAKE SOURCES

or when the data and other information available are very limited, a description of the earthquake source as an area source may be considered. In the case where the source is located at a distance from the site greater than two times the focal depth h, the shape of the source is not important [15]. Thus, the shape for the area source is assumed to be circular with its center on the site, and earthquake occurrences are taken as uniformly distributed over this area. As a result, any earthquake that may occur outside the defined circular area is considered to have a negligible effect on the slope.

In Appendix B are given the analytical expressions of the probability distributions of the maximum acceleration for the three types (i.e., point, line and area) of earthquake source.

2.4 Probability Distribution of the Maximum Horizontal Ground Acceleration (Point Source)

From Equation (2-10), one has that $a_{max} = a_{max}(m)$ is a monotonic function of magnitude m, the probability density function of which is given by Equation (2-9). Using the concept of transformation of variables [20], the distribution of a_{max} can be obtained as

$$f(a_{max}) = \frac{f_m(m)}{\left| \frac{da_{max}(m)}{dm} \right|} \tag{2-14}$$

where a_{max} substituted for m in $f_m(m)$, and $\left|\frac{da_{max}(m)}{dm}\right|$ is the absolute value of the derivative of a_{max} with respect to m. The latter is found from Equation (2-12) to be equal to

$$\left|\frac{da_{max}(m)}{dm}\right| = b_1 b_2 e^{b_2 m} (R+b_4)^{-b_3} = b_2 a_{max} \tag{2-15}$$

Combining Equations (2-9), (2-14) and (2-15), it is found that

$$f(a_{max}) = \frac{k}{b_2} \cdot \frac{1}{a_{max}} \exp[-\beta(m-m_o)]$$

Solving Equation (2-12) for m and substituting into the above expression, one has that the probability density function of the maximum horizontal ground acceleration is equal to

$$f(a_{max}) = \frac{k}{b_2} \cdot \frac{1}{a_{max}} \exp[-\beta(\frac{1}{b_2} \ln \frac{a_{max}}{b_1(R+b_4)^{-b_3}} - m_o)] \tag{2-16}$$

The range of variation of a_{max} can be found by introducing the lower and upper limits of magnitude m into Equation (2-12). Thus,

$$b_1 e^{b_2 m_o} (R+b_4)^{-b_3} \leq a_{max} \leq b_1 e^{b_2 m_1} (R+b_4)^{-b_3} \qquad (2\text{-}17)$$

The two attenuation relationships that have been suggested for the Northeastern United States (Table 4) are as follows:

$$a_{max} = 1100\ e^{0.5m} (R+25)^{-1.32} \qquad \text{(Case 1)} \qquad (2\text{-}18)$$

$$a_{max} = 1.183\ e^{1.15m} R^{-1.0} \qquad \text{(Case 2)} \qquad (2\text{-}19)$$

where m is a random variable the frequency distribution of which is given by Equation (2-9).

In Figures 12 and 13 are shown the frequency and cumulative distributions of a_{max} found using Equation (2-18) (Case 1) and in Figures 14 and 15 are shown the same quantities that correspond to Equation (2-19) (Case 2).

When the error term ε is considered, the expressions of the attenuation relationships given by Equations (2-18) and (2-19), become

$$a_{max} = 1100\ e^{0.5m} (R+25)^{-1.32} \varepsilon \qquad \text{(Case 1)} \qquad (2\text{-}20)$$

$$a_{max} = 1.183\ e^{1.15m} R^{-1.0} \varepsilon \qquad \text{(Case 2)} \qquad (2\text{-}21)$$

where ε is log-normally distributed with median and standard deviation equal to 1.0 and 0.5, respectively.

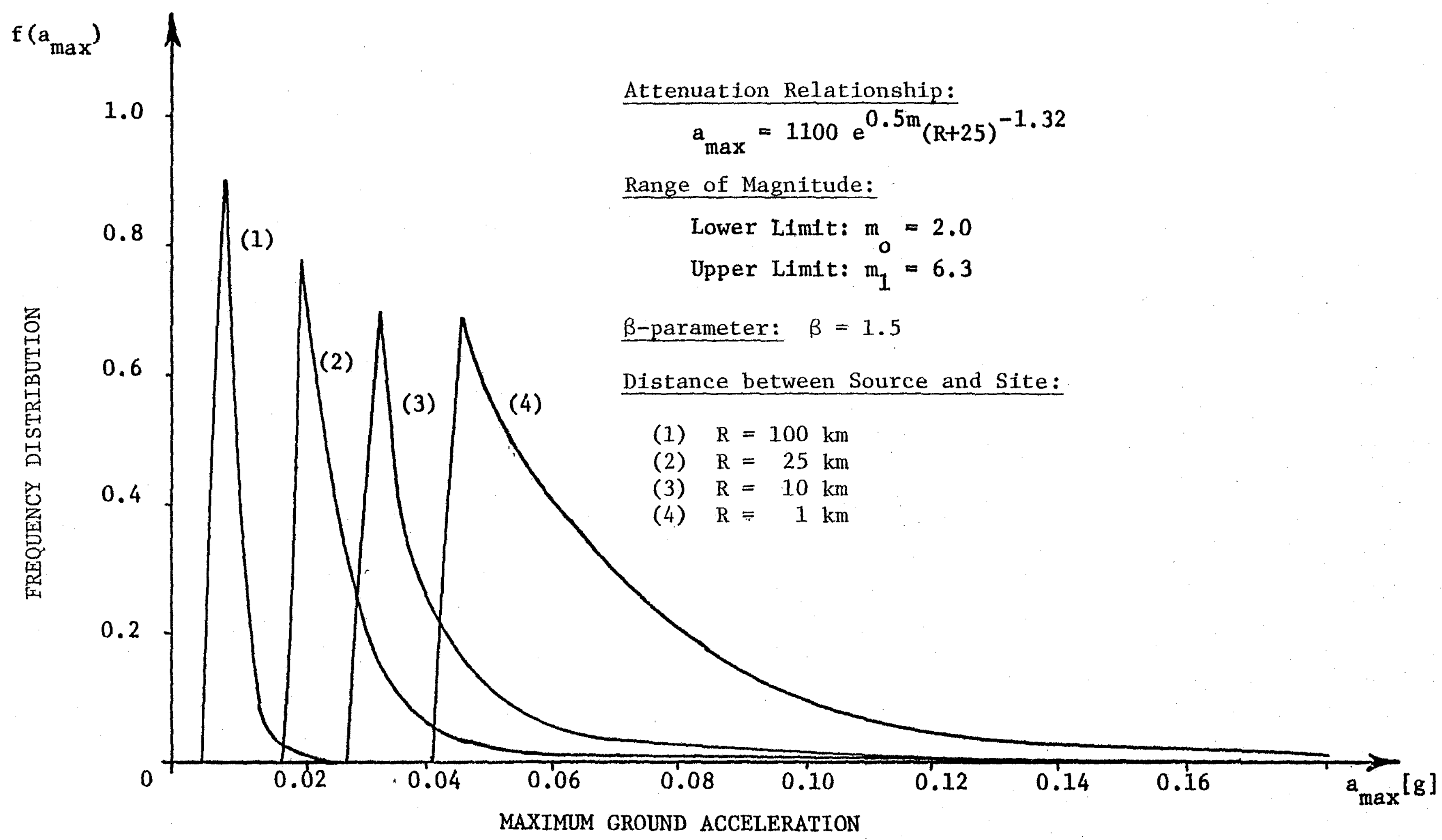

FIGURE 12. FREQUENCY DISTRIBUTION OF MAXIMUM GROUND ACCELERATION (CASE 1)

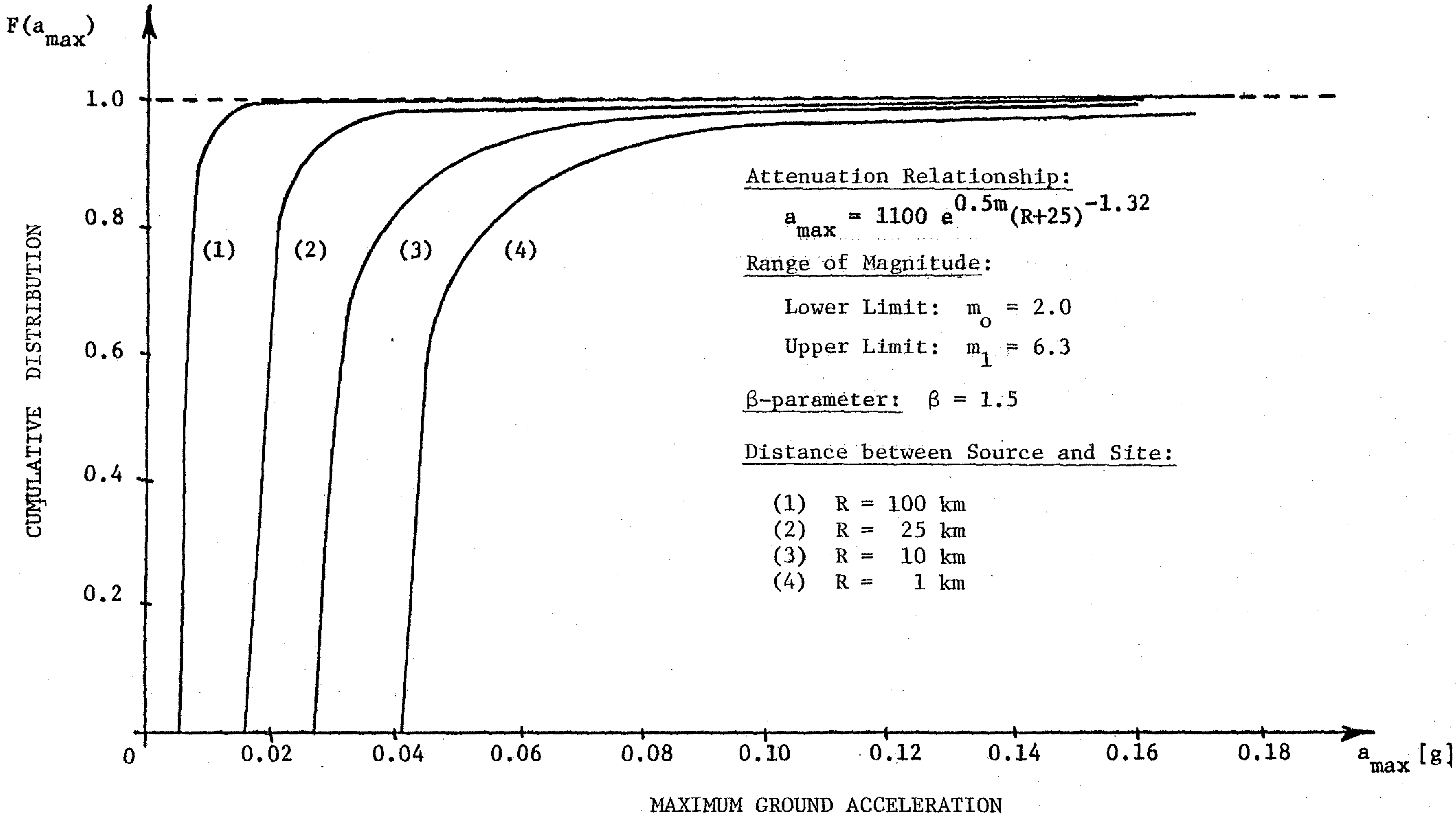

FIGURE 13. CUMULATIVE DISTRIBUTION OF MAXIMUM GROUND ACCELERATION (CASE 1)

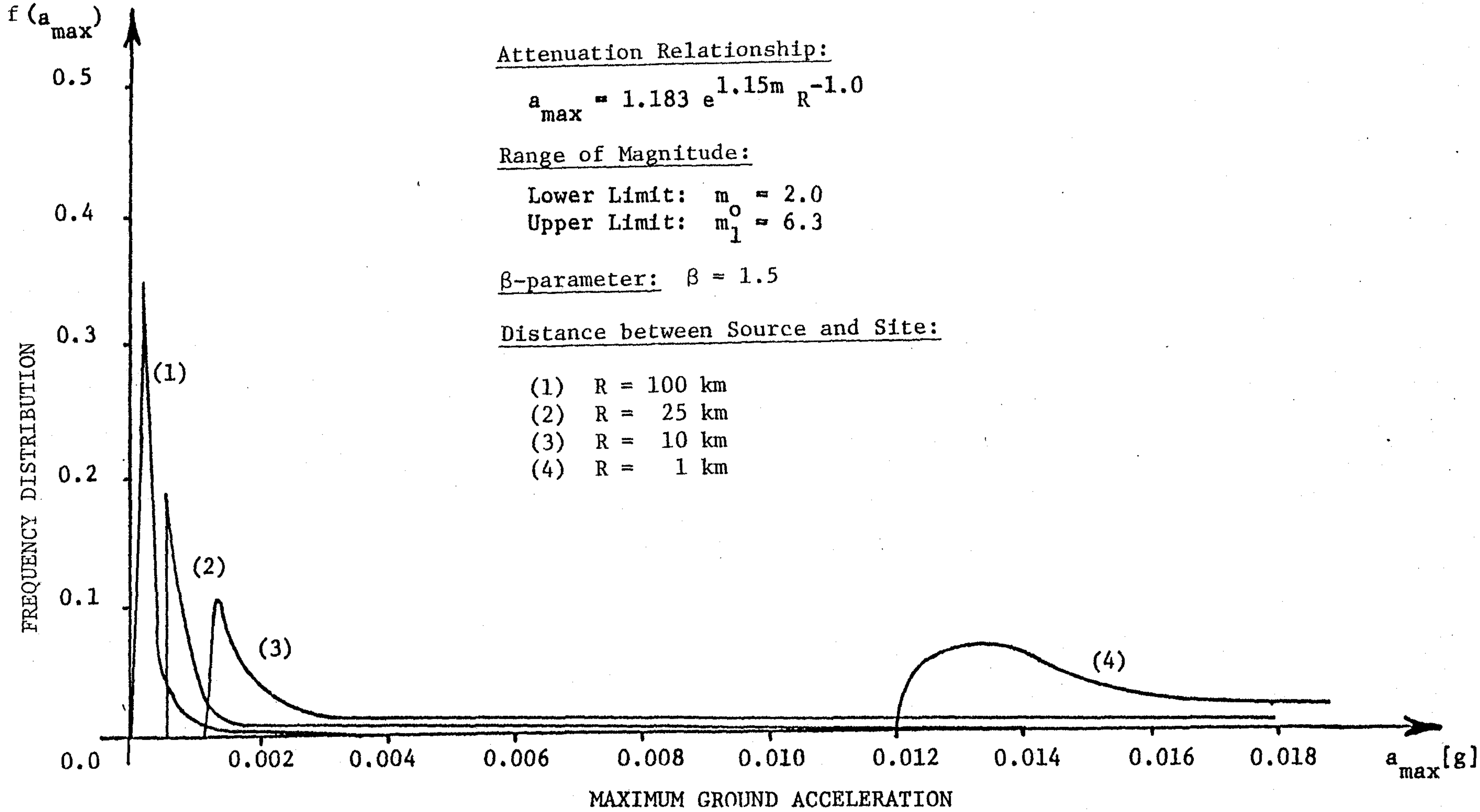

FIGURE 14. FREQUENCY DISTRIBUTION OF MAXIMUM GROUND ACCELERATION (CASE 2)

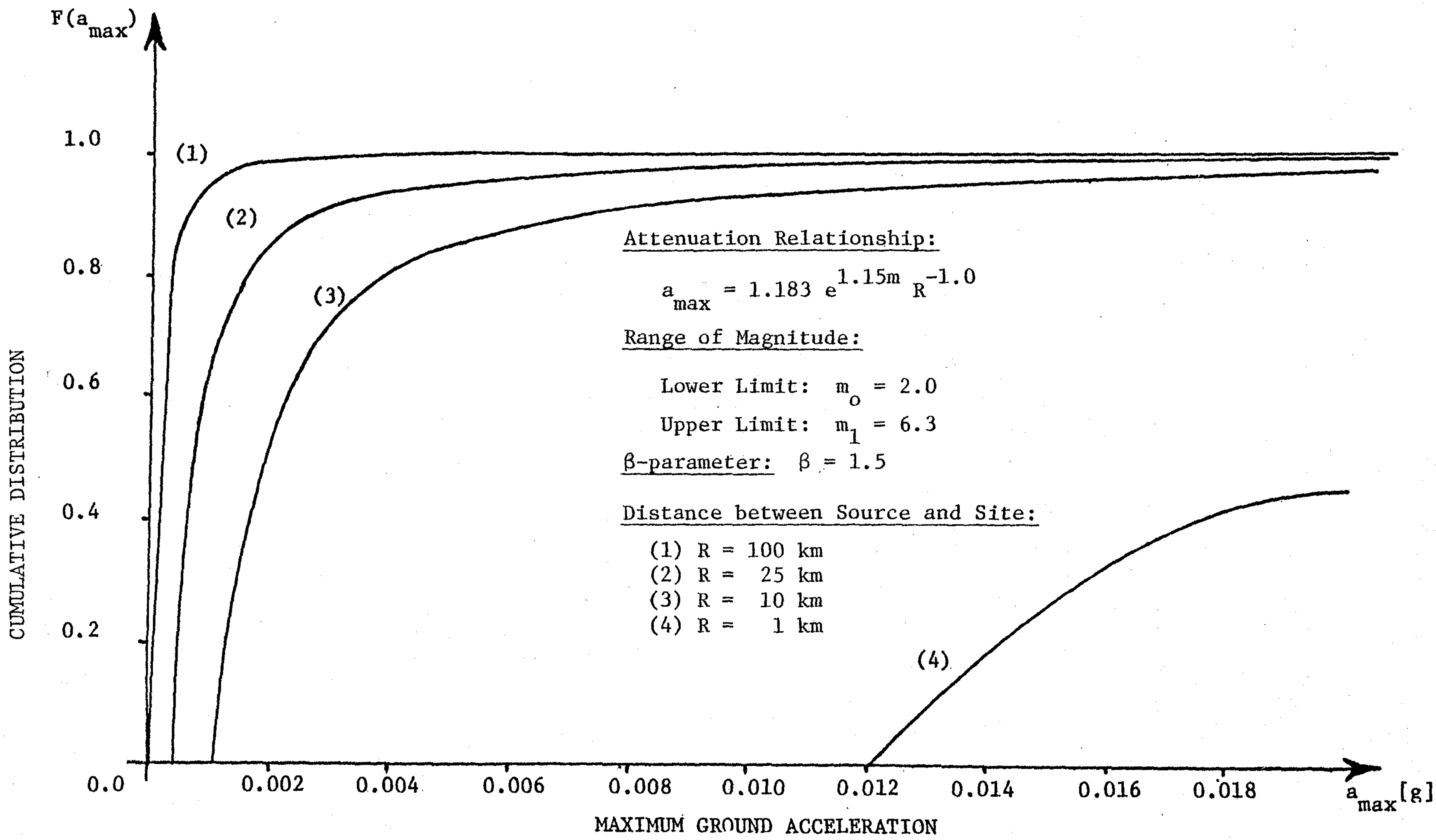

FIGURE 15. CUMULATIVE DISTRIBUTION OF MAXIMUM GROUND ACCELERATION (CASE 2)

In Figures 16 and 17 are shown the frequency and cumulative distribution of a_{max} that correspond to Equation (2-20) (Case 1) while in Figures 18 and 19 are shown the same quantities that correspond to Equation (2-21) (Case 2).

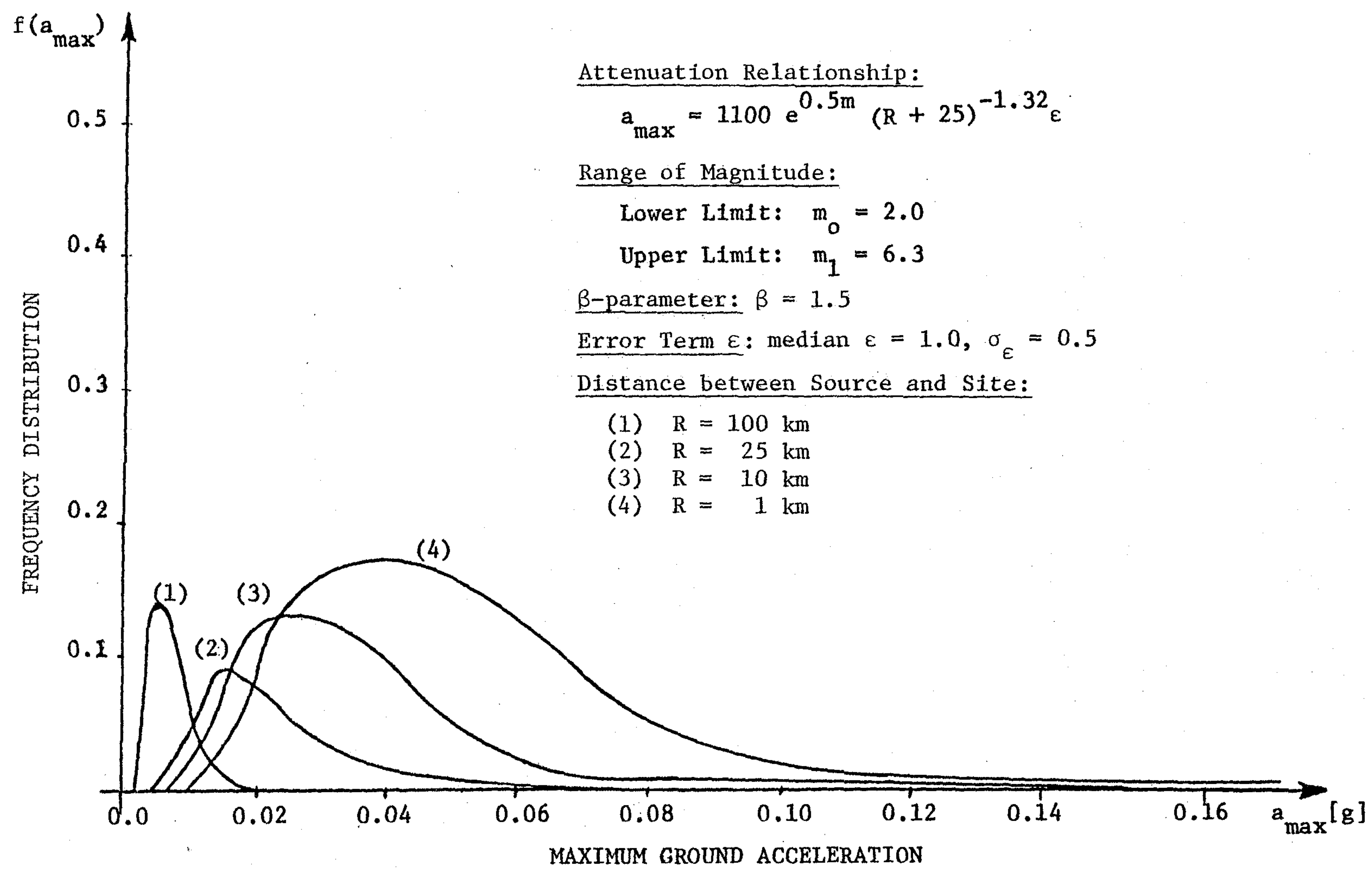

FIGURE 16. FREQUENCY DISTRIBUTION OF MAXIMUM GROUND ACCELERATION (WITH ERROR TERM - CASE 1)

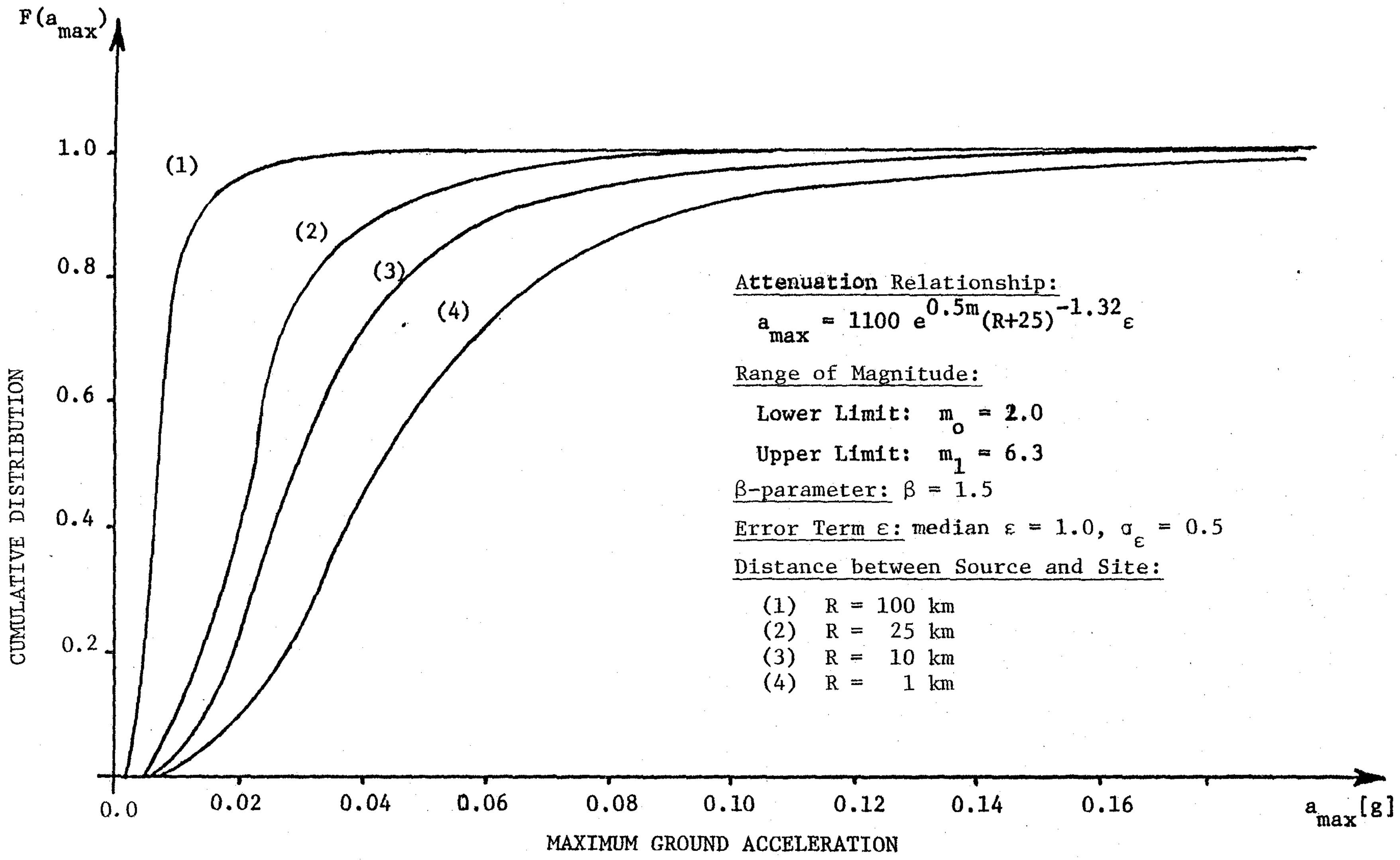

FIGURE 17. CUMULATIVE DISTRIBUTION OF MAXIMUM GROUND ACCELERATION (WITH ERROR TERM - CASE 1)

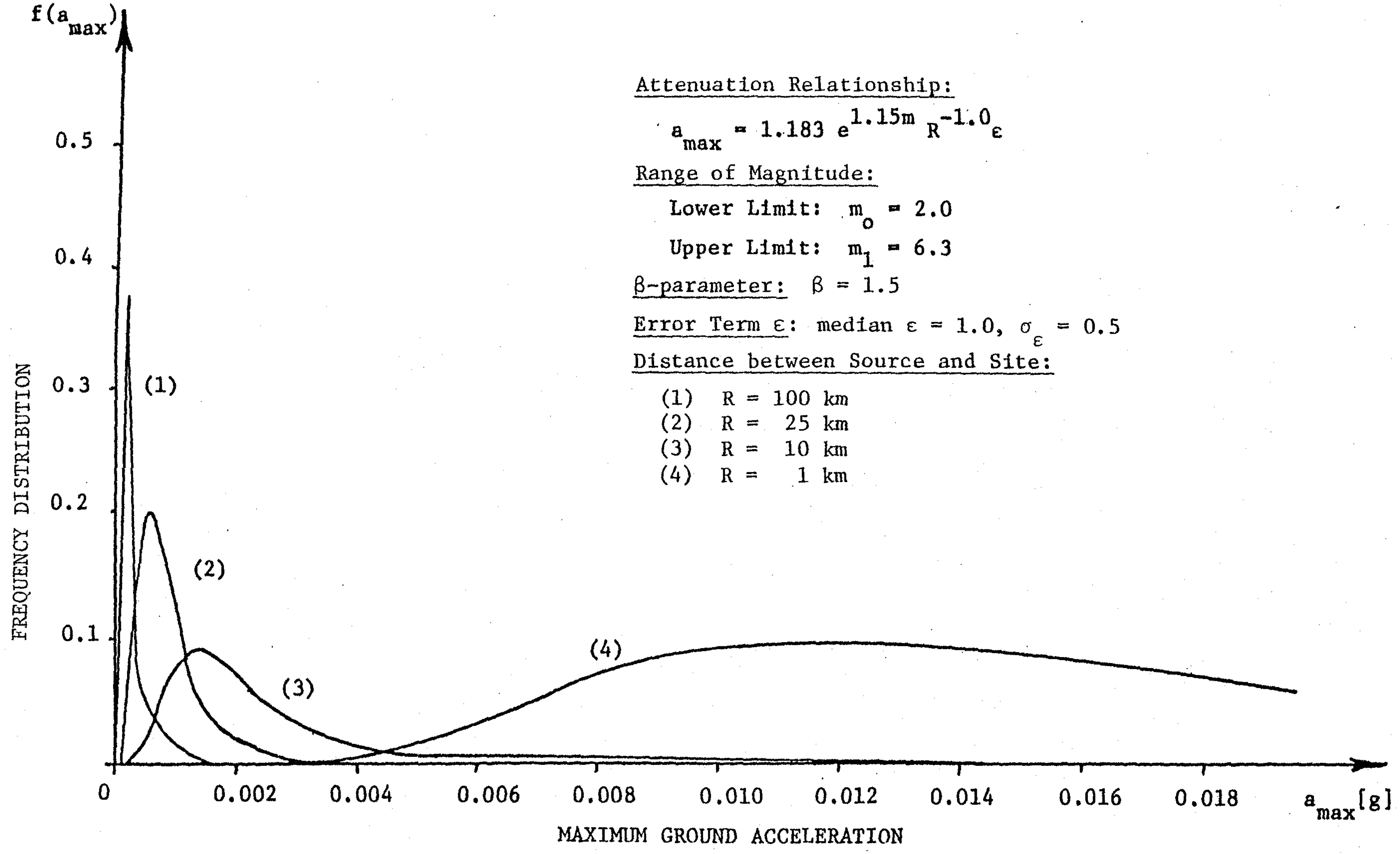

FIGURE 18. FREQUENCY DISTRIBUTION OF MAXIMUM GROUND ACCELERATION (WITH ERROR TERM - CASE 2)

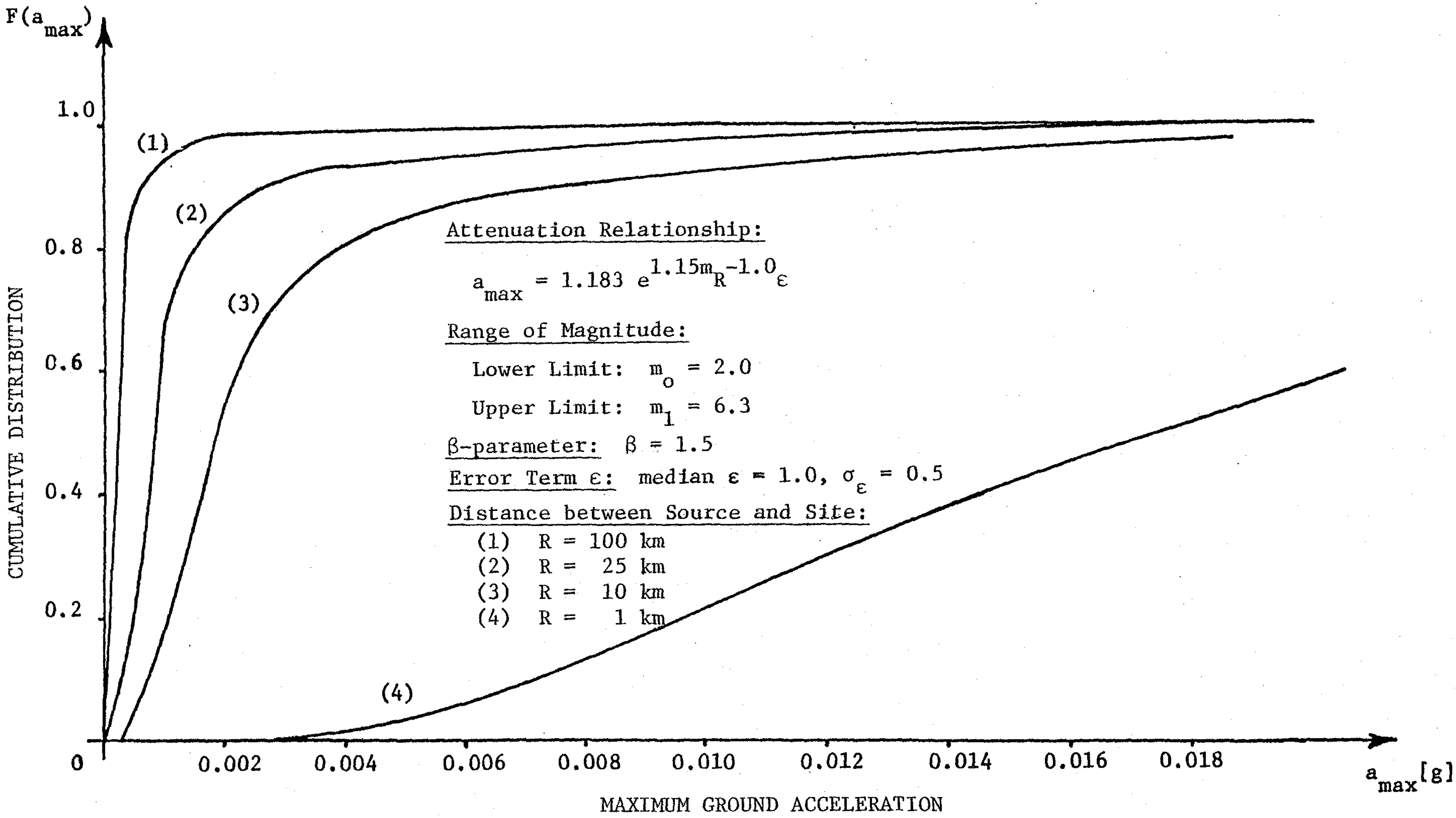

FIGURE 19. CUMULATIVE DISTRIBUTION OF MAXIMUM GROUND ACCELERATION (WITH ERROR TERM - CASE 2)

2.5 Statistical Values of Maximum Horizontal Ground Acceleration (Point Source)

The exact values of the mean $\bar{a}_{max}$ and variance $Var(a_{max})$ of the maximum horizontal acceleration are equal to

$$\bar{a}_{max} = \int a_{max}\ f(a_{max})\ da_{max}$$
$$\qquad (2\text{-}22)$$
$$Var(a_{max}) = \int (a_{max} - \bar{a}_{max})\ f(a_{max})\ da_{max}$$

where $f(a_{max})$ is given by Equation (2-16), and the limits of the integrations are given by Equation (2-17).

A convenient and yet accurate way to obtain the statistical values of a_{max} is to apply the Monte Carlo technique using Equation (2-12). This procedure involves the selection of a large number of values for the random variable m from its cumulative distribution F(m), given by Equation (2-8). These values are then substituted into Equation (2-18) and the corresponding values of a_{max} are collected and analyzed statistically to obtain $\bar{a}_{max}$ and $Var(a_{max})$.

An estimate of $\bar{a}_{max}$ and $Var(a_{max})$ can also be obtained through a Taylor series expansion of the function $a_{max}(m)$ around the value $a_{max}(\bar{m})$, where $\bar{m}$ is the mean value of the magnitude. Thus,

$$\bar{a}_{max} \cong a_{max}(\bar{m}) + \frac{1}{2}\ \frac{\partial^2 \bar{a}_{max}}{\partial m^2}\ Var(m)$$
$$\qquad (2\text{-}23)$$
$$Var(a_{max}) \cong \left(\frac{\partial \bar{a}_{max}}{\partial m}\right)^2\ Var(m)$$

where $\bar{a}$ in the derivatives denotes that the latter are evaluated at the mean value $\bar{m}$ of magnitude m.

After the derivatives of a_{max} are obtained from Equation (2-12) and introduced into Equations (2-23), the latter become

$$\bar{a}_{max} \cong \frac{b_1 e^{b_2 \bar{m}}}{(R+b_4)^{b_3}} [1 + \frac{1}{2} b_2^2 \, Var(m)]$$

$$Var(a_{max}) \cong [\frac{b_1 b_2 e^{b_2 \bar{m}}}{(R+b_4)^{b_3}}]^2 \, Var(m) \qquad (2\text{-}24)$$

where the mean value $\bar{m}$ and the variance Var(m) of magnitude m are given by Equations (2-11).

In Table 5 are listed the mean value $\bar{a}_{max}$, standard deviation $S_{a_{max}}$ and coefficient of variation $V_{a_{max}}$ of the maximum horizontal ground acceleration for a point source and for the two attenuation relationships, given by Equations (2-18) and (2-19), respectively.

In Figures 20 and 21 is shown the expected value of the maximum acceleration as a function of distance R for the two attenuation relationships. For comparison purposes, in the same figures are shown the results for the case where a more critical range of variation for the magnitude m is assumed (i.e., $4.0 \leq m \leq 8.0$).

TABLE 5. STATISTICAL VALUES OF MAXIMUM HORIZONTAL GROUND ACCELERATION (POINT SOURCE)

ATTENUATION RELATIONSHIP*	DISTANCE	MONTE CARLO SIMULATION			TAYLOR SERIES EXPANSION		
	R [km]	$\bar{a}_{max}$ [g]	$\sigma_{a_{max}}$ [g]	$V_{a_{max}}$ (%)	$\bar{a}_{max}$ [g]	$\sigma_{a_{max}}$ [g]	$V_{a_{max}}$ (%)
CASE 1	1	0.0594	0.0244	41.08	0.0605	0.0185	30.58
	10	0.0410	0.0176	42.93	0.0408	0.0125	30.64
	25	0.0256	0.0110	42.97	0.0255	0.0078	30.59
	100	0.0075	0.0031	41.33	0.0076	0.0023	30.26
	200	0.0035	0.0015	42.86	0.0041	0.0013	31.71
CASE 2	1	0.0355	0.0684	192.68	0.0327	0.0190	58.10
	10	0.0040	0.0077	192.50	0.0033	0.0019	57.58
	25	0.0016	0.0031	193.75	0.0013	0.0008	61.54
	100	0.0004	0.0007	175.00	0.0003	0.0002	66.67
	200	0.0002	0.0004	200.00	0.0002	0.0001	50.00

*CASE 1: $a_{max} = 1100\ e^{0.5m}(R+25)^{-1.32}$

CASE 2: $a_{max} = 1.183\ e^{1.15m}\ R^{-1.0}$

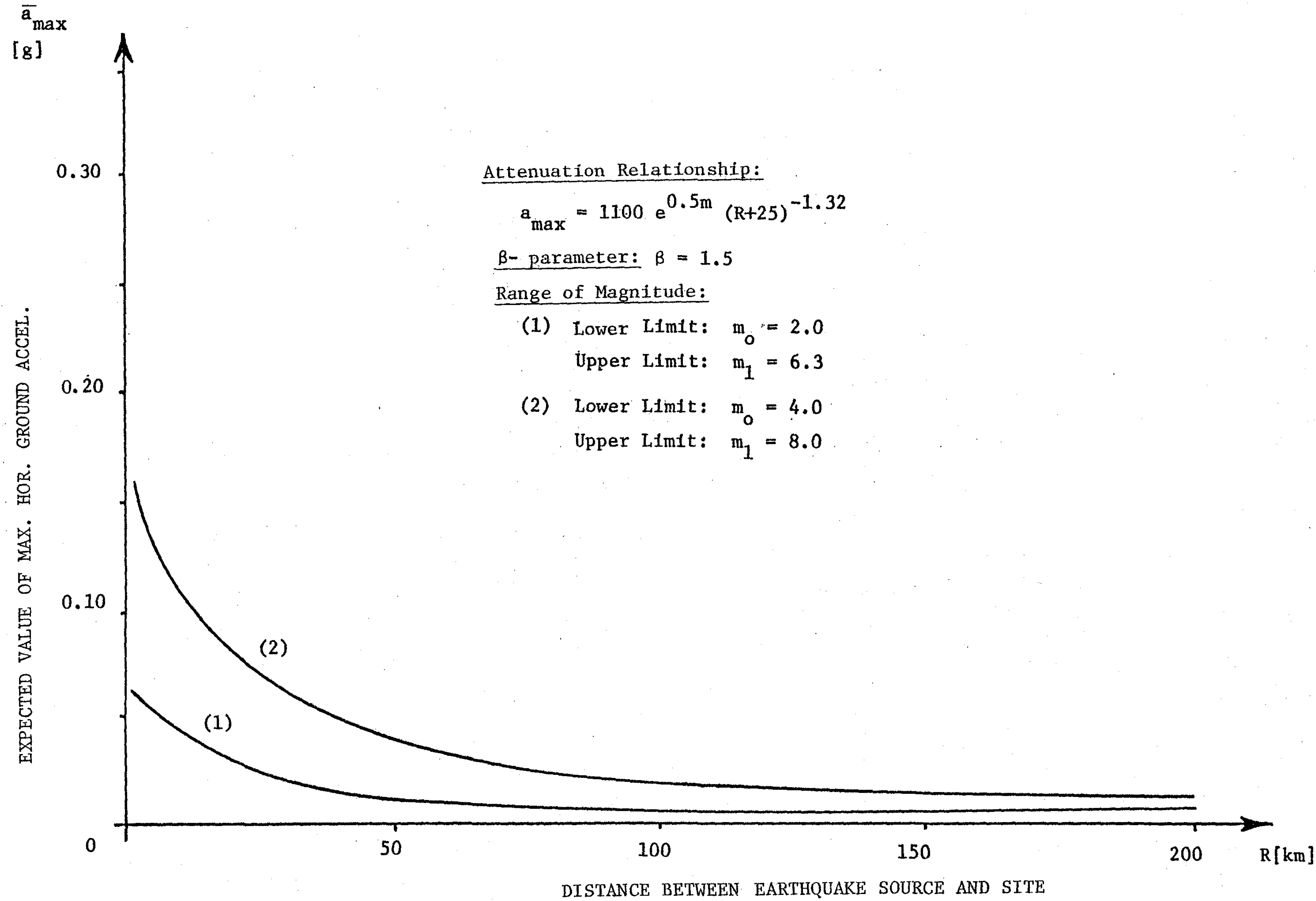

FIGURE 20. RELATIONSHIP BETWEEN $\overline{a}_{max}$ AND DISTANCE R (CASE 1)

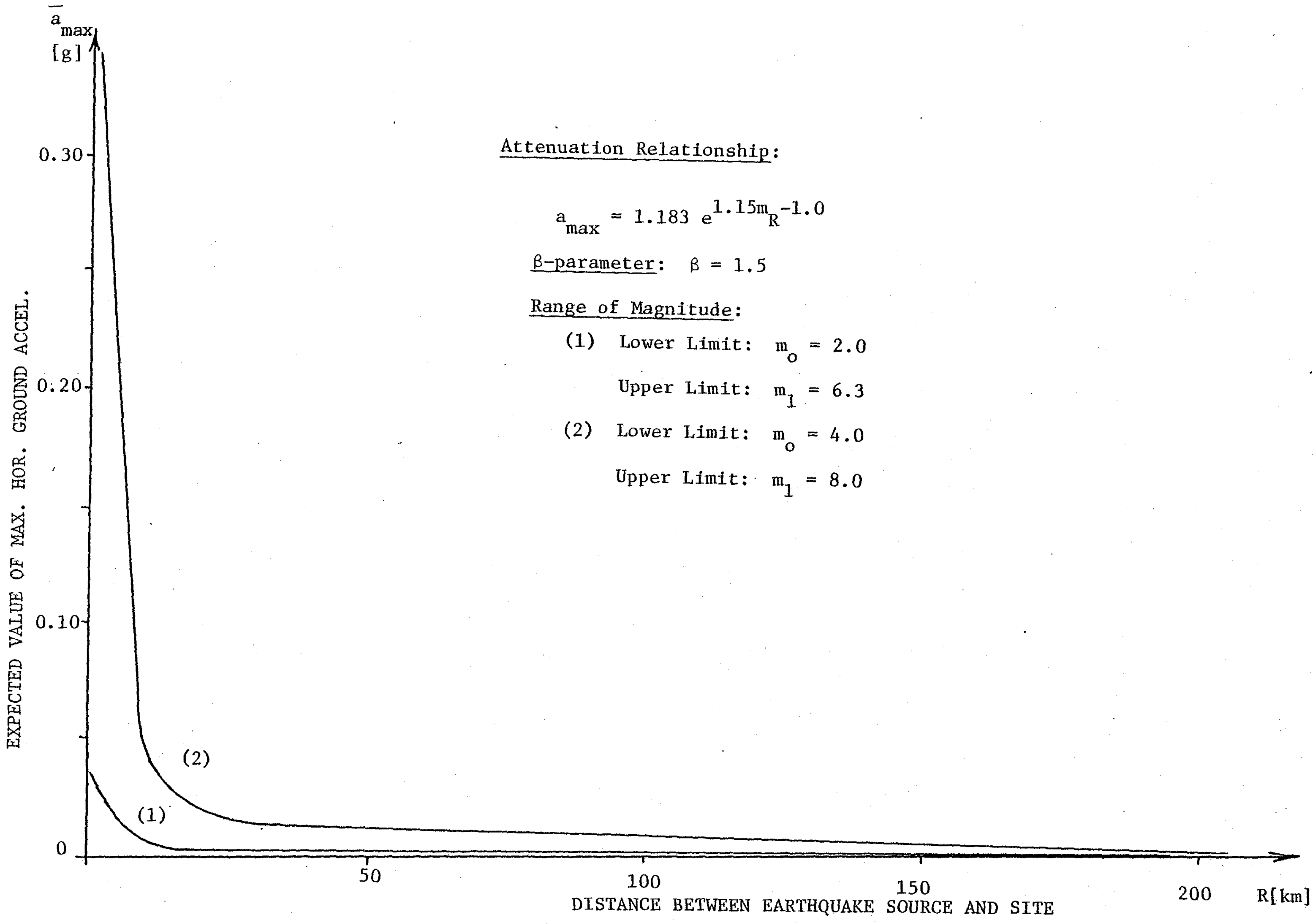

FIGURE 21. RELATIONSHIP BETWEEN $\bar{a}_{max}$ AND DISTANCE R (CASE 2)

The influence of the β-parameter (see Equation 2-9) on the expected value $\overline{a}_{max}$ of the maximum ground horizontal ground acceleration is shown in Figures 22 and 23. Figure 22 corresponds to Equation (2-18) while Figure 23 to Equation (2-19).

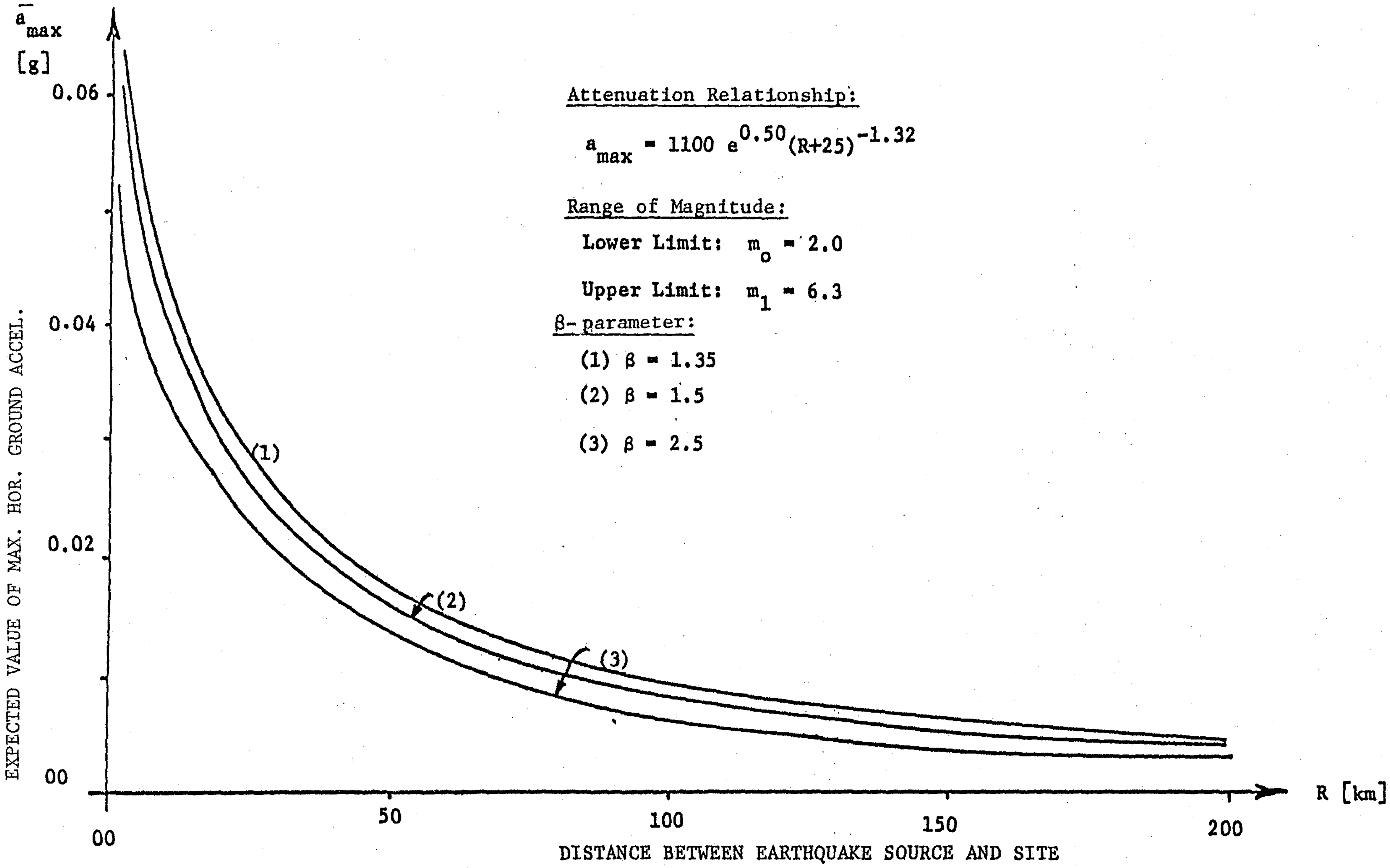

FIGURE 22. RELATIONSHIP BETWEEN $\bar{a}_{max}$ AND DISTANCE R FOR VARIOUS VALUES OF β-PARAMETER (CASE 1)

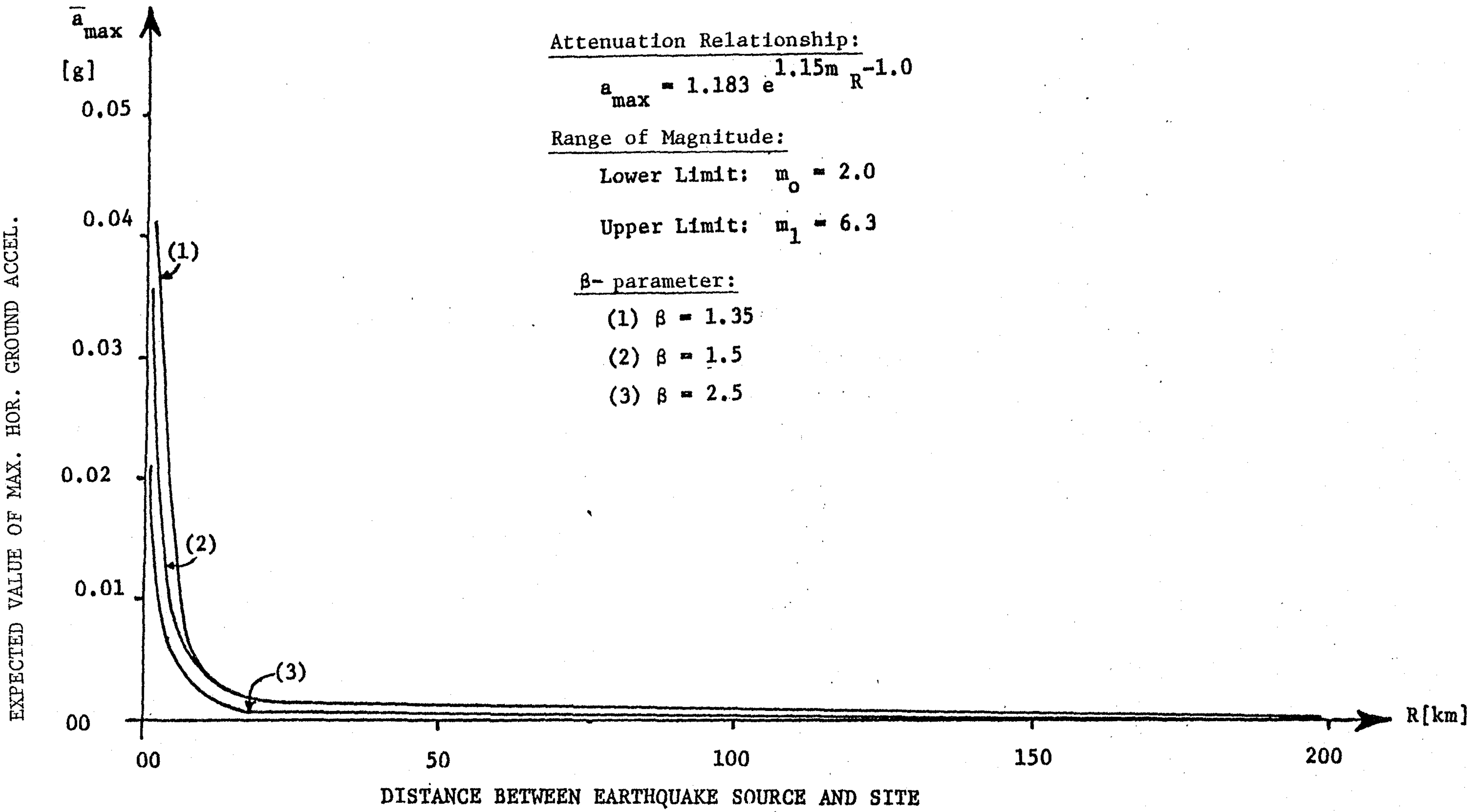

FIGURE 23. RELATIONSHIP BETWEEN $\bar{a}_{max}$ AND DISTANCE R FOR VARIOUS VALUES OF β-PARAMETER (CASE 2)

3. DISCUSSION

In a conventional seismic or static stability analysis, the safety of a soil slope is measured by means of a factor of safety FS. Material and seismic parameters entering the expression for FS are conventionally treated as single-valued quantities. However, soil properties (e.g., c and ϕ) and ground motion parameters (i.e., a_{max}) are generally random variables, the variability of which lend themselves to a probabilistic formulation of the stability problem. A pseudo-static, probabilistic model, as employed in the present work, is capable of accounting for (a) the variability in the numerical values of the material strength parameters, (b) the uncertainty in the location of the failure surface inside the soil slope, and (c) the uncertainty in the exact value of the seismic load.

The soil material comprising the slope was assumed to be statistically homogeneous with strength parameters c and t (=tanϕ) along potential failure surfaces being identically distributed random variables with given mean values ($\bar{c}, \bar{t}$) and coefficients of variation (V_c, V_t). Following results found by previous investigators, the probability distributions of c and t were assumed to follow the beta (or, Pearson's type I) model.

Potential failure surfaces were taken to be of a log-spiral type and were defined with the aid of three random variables: strength parameter t and two geometric parameters h_o and θ_o. The statistical values and bounds of h_o and θ_o were determined empirically, taking advantage of previous experience with log-spiral types of surfaces. Thus, generated failure surfaces were within a realistic range (Figure 2). In Section 1.3, a procedure was presented for an approximate determination of the most probable (mean) failure surface. For the slope considered in the illustrative example (Figure 3), it was found that, by neglecting the variances of the three random variables (h_o, θ_o, t), the corresponding failure surface (see Equation 1-8a) lay very close to the mean surface.

The safety of the slope was measured in this study in terms of its probability of failure p_f, the numerical values of which were obtained through a Monte Carlo simulation of failure. In Figure 7 was given the flow-chart of the operations followed during the simulation. After values of the random variables were selected from their distributions, the resisting (R) and driving (S) forces were calculated and compared. Thus, failure corresponded to the case wherein R was exceeded by S ($R < S$). This procedure was repeated a large number of times and the probability of failure p_f was obtained as the ratio of the number of counted failures M over the total number of repetitions N(p_f=M/N). Implied in this method was a frequency interpretation of the probability (p_f) of a random event ("failure") in a specified random experiment (generation of a failure surface and comparison of the resulting values of R and S). In his discussion on the precision of the frequency interpretation of probability, Papoulis [32, p. 4] stated: "This interpretation is obviously imprecise; however, it cannot be essentially improved ... probability, like any physical theory is related to physical phemomena only in inexact terms. Nevertheless, the theory is an exact discipline developed logically from clearly defined axioms, and when it is applied to real problems, it works". Furthermore, as in the developed procedure the selection of failure surfaces was limited to those passing through the toe, the resulting value of the probability of failure may be considered as an upper bound.

It should be noted that this study did not attempt a "system" approach to the reliability of slopes. Such an approach, in which the slope is considered as a series system with infinite components (potential failure surfaces), has been pursued in the past by Catalan and Cornell [11] who provided an approximate formulation of slope stability by transforming the slope reliability problem into a level-crossing one. The authors remarked that "the conceptulization of a slope as a series system with infinitely many distinct, but correlated modes was not found to be the most fruitful approach".

In the present analysis, the resistance R developed along a potential failure surface was assumed to be constant during the earthquake loading. This is a reasonable assumption for a wide variety of soils, particularly cohesive ones [3]. The proposed approach is not directly applicable to the analysis of soil slopes when the material's strength decreases during the cyclic loading. This could be, for example, the case of liquefaction of saturated sands or sensitive clays [3]. The applicability and limitation of the above assumption has been also recognized by other researchers of the subject: "Because of these difficulties, it is not at the present time possible to make an accurate determination of the behavior of soils (cohesionless soils and sensitive clays) which are susceptible to liquefaction-like phenomena ... Fortunately, not all soils are susceptible to such phenomena. For many soils, the resistance to shear is largely unaffected by repeated cycles of loading" [48].

The seismic load was introduced into the present analysis through the maximum acceleration experienced by the slope mass during an earthquake. The maximum horizontal acceleration of the slope was taken to be identical to that of the ground (rigid body assumption). Furthermore, it was assumed that the magnitude of the vertical component (with an upward direction) of the maximum acceleration was equal to two-thirds of that of the horizontal component (with a direction away from the slope) [43]; and that both components acted on the slope mass simultaneously.

Three types of factors have an affect on ground motion parameters, in general, and maximum ground acceleration, in particular. These are (a) source related factors, (b) travel path related factors, and (c) factors reflecting site conditions. The current state-of-the-art is limited to considering only a few representatives from each type [22]. Thus, in the present study, source factors were accounted through the earthquake magnitude, travel path factors through the distance between source and site, and local factors through a number of regional parameters.

Comparisons between observed and computed values of the maximum horizontal acceleration have indicated that their ratio (the "error term ε") follows closely a log-normal distribution. When the "error term ε" was included in the present study, the two attenuation relationships received the expressions given in Equations (2-20)(Case 1) and (2-21)(Case 2). The frequency and cumulative distributions of a_{max} were obtained for a median and standard deviation of ε equal to 1.0 and 0.5, respectively. These are shown in Figures 16 and 17 for Case 1 and in Figures 18 and 19 for Case 2.

Three types of earthquake sources were considered (Figure 11); namely, (a) a point source, (b) a line (or, fault) source, and (c) an area source. A point source (Figure 11a) constitutes the fundamental type of earthquake source. A line source (Figure 11b) is used if a fault has been clearly identified in a certain region, or if a string of earthquakes occurred over a period of time along a well defined line. An area source (Figure 11c) is used when the earthquakes that have occurred at a certain site are almost uniformly distributed over an area, or when there is very limited seismic data and other information [16].

In the case of a point source, the frequency $f(a_{max})$ and cumulative $F(a_{max})$ distributions of the maximum horizontal acceleration a_{max} were derived from the distribution of the magnitude by a transformation of variables (Section 2.4). The expressions for $f(a_{max})$ and $F(a_{max})$ for the line and area sources were given in Appendix B. In Appendix B were also given the expressions for $f(a_{max})$ and $F(a_{max})$ for the case of a log-quadratic frequency-magnitude relationship (for point source).

The statistical values of the maximum horizontal acceleration were found through a Monte Carlo simulation for the two attenuation relationships used, given by Equations (2-18)(Case 1) and (2-19)(Case 2), and for a range of values for the distance R (point source). The results were listed in Table 5, from which it can be seen that the expected values of a_{max} were always higher in Case 1 than in Case 2. The opposite was true for the coefficient of variation $V_{a_{max}}$ of a_{max}. In Table 5 were also listed the estimates for the statistical values of a_{max} that were obtained through a Taylor series expansion (see Equations 2-23). From a comparison of the results, it can be seen that the expected values of a_{max} for the two cases were very similar while the values of the standard deviations found through the Taylor series expansion were much lower.

In order to examine the importance of the limits (m_o, m_1) of the magnitude m on the expected value of the maximum horizontal acceleration, the latter was determined for two sets of limiting values of m: one, for $m_o = 2.0$, $m_1 = 6.3$ (pertinent to New York State), and, another, for $m_o = 4.0$ and $m_1 = 8.0$. The results are shown in Figures 20 (Case 1) and 21 (Case 2), from which it can be seen that for the more critical range of magnitude, the expected values of a_{max} are considerably higher.

The magnitude of an earthquake was considered as random variable the frequency and cumulative distributions of which were derived in Section 2.2 and were given by Equation (2-7) and (2-8), respectively. These expressions correspond to a log-linear frequency-magnitude relationship. The case of a log-quadratic frequency-magnitude relationship was also examined and the results were presented in Appendix A.

A reasonable range of variation for the earthquake magnitude m in New York State has been found [31] to be between $m_o = 2.0$ and $m_1 = 6.3$ ($2.0 \leq m \leq 6.3$). The same range of variation for m was also adopted in the present study. The influence of the β-parameter (see Equation 2-2) on the frequency f(m) distributions of magnitude m was examined for three values of β; namely, $\beta = 1.35$, 1.5 and 2.5. The results were shown in Figures 9 and 10, from which one has that f(m) and F(m) are not affected much when β varies between 1.35 and 1.50 (a range that corresponds to the Northeastern United States [31]). A value of $\beta = 2.50$, however, resulted to considerable differences in the two distributions.

Two different attenuation relationships that have been proposed for the Northeastern United States were used to obtain the maximum horizontal ground acceleration a_{max} as a function of the earthquake magnitude, the distance between the source and the site and a number of regional parameters. These were given by Equations (2-18) (Case 1) and (2-19) (Case 2). The frequency and cumulative distributions of a_{max} that correspond to each of the two attenuation relationships are shown in Figures 12 and 13 (Case 1) and 14 and 15 (Case 2), respectively.

Finally, the influence of the β-parameter (see Equation 2-2) on the expected value $\bar{a}_{max}$ of a_{max} was also examined and the results were shown in Figures 23 (Case 1) and 24 (Case 2). It can be seen that, for both cases, a smaller value of the β-parameter resulted to a higher value of $\bar{a}_{max}$.

4. SUMMARY

A model was developed to determine the reliability of earth slopes subjected to earthquake loading. The material comprising the slope was assumed to be probabilistically homogeneous with strength parameters being random variables following a beta distribution. Potential failure surfaces were considered to be of an exponential shape (log spiral) and were defined with the aid of three random variables: two geometric and one strength parameters. The seismic load was introduced through the maximum acceleration (a_{max}) experienced by the slope during an earthquake. The statistical characteristics of a_{max} were determined by exploring the dependence of the latter on such factors as the earthquake magnitude, the type of earthquake source and the location of the slope. The measure used to assess the reliability of a soil slope was its probability of failure the numerical values of which were determined through a Monte Carlo simulation.

5. LIST OF REFERENCES

1. Alonso, E.E., "Risk Analysis of Slopes and Its Application to Slopes in Canadian Sensitive Clays", Geotechnique 26, No. 3, pp. 453-472, 1976.

2. Alonso, E.E., "Stochastic Formulation of Soil Properties", Proc. 2nd Inter. Conf. Applic. of Stat. and Probab. in Soil and Struct. Engin., Aachen, W. Germany, pp. 9-32, 1975.

3. Arango I. and Seed, H.B., "Seismic Stability and Deformation of Clay Slopes", Journal of Geot. Engin. Div., ASCE, GT2, pp. 139-156, 1974.

4. Athanasiou-Grivas, D., "Reliability Analysis of Retaining Structures", Proc. 3rd Inter. Conf. on Appl. of Stat. and Probab. to Soil and Struct. Engin., Sydney, Australia, Jan. 1979.

5. Athanasiou-Grivas, D., "Program RASSUEL-Reliability Analysis of Soil Slopes under Earthquake Loading", Report No. CE-78-6, Dept. of Civ. Engin., RPI, Troy, N.Y., December 1978.

6. Athanasiou-Grivas, D., "Reliability of Slopes of Particulate Materials", Ph.D. Thesis, Purdue University, 1976.

7. Athanasiou-Grivas, D. and Harr, M.E., "Stochastic Propagation of Rupture Surfaces Within Slopes", Proc. 2nd Inter. Conf. on Appl. of Stat. and Probab. to Soil and Struct. Engin., Aachen, W. Germany, pp. 33-54, 1975.

8. Baker, R. and Garber, M., "Variational Approach to Slope Stability Proc. 9th Inter. Conf. on Soil Mech. and Found. Engin., Tokyo, Japan, Vol. 2, pp. 9-12, July 1977.

9. Bishop, A.W. and Morgenstern, N.R., "Stability Coefficients for Earth Slopes", Geotechnique, 10, pp. 129-150, 1960.

10. Boutrup, E. and Lovell, C.W., "Searching Techniques in Slope Stability Analysis", Proc. 15th Ann. Meet. of the Soc. of Eng. Sci., Gainesville, Florida, pp. 447-452, Dec. 1978.

11. Catalan, M.J. and Cornell, C.A., "Earth Slope Reliability by a Level-Crossing Method", Journal of Geot. Div., ASCE, GT6, pp. 591-604, June 1976.

12. Chen, W.F., Limit Analysis and Soil Plasticity, Elsevier Scientific Publishing Co., Netherlands, 1975.

13. Chowdhury, R.N., Slope Analysis, Elsevier Scientific Publishing Co., Netherlands, 1978.

14. Collin, A., "Landslides in Clays", (Translated by W.R. Schriever, 1956), Univ. of Toronto Press, 1840.

15. Cornell, C.A. and Vanmarcke, E.H., "The Major Influences on Seismic Risk", Proc. 4th World Conf. on Earthquake Engin., Vol. A-1, pp. 69-83, 1969.

16. Cornell, C.A., "Engineering Seismic Risk Analysis", Bull. of Seism. Soc. of Amer., Vol. 58, No. 5, pp. 1583-1606, October 1968.

17. Duncan, J.M. and Wright, S.G., "The Accuracy of Equilibrium Analyses of Slope Stability", Proc. 15th Ann. Meet. of the Soc. of Eng. Sci., Gainesville, Florida, pp. 207-212, Dec. 1978.

18. Frölich, O.K., "The Factor of Safety with Respect to Sliding of a Mass of Soil Along the Arc of a Logarithmic Spiral", Proc. 3rd Inter. Conf. on Soil Mech. and Found. Engin., Switzerland, Vol. 2, pp. 230-233, 1953.

19. Hahn, G.J. and Shapiro, S.S., Statistical Models in Engineering, Wiley, N.Y., 1967.

20. Harr, M.E., Mechanics of Particulate Materials - A Probabilistic Approach, McGraw-Hill, N.Y., 1977.

21. Höeg, K. and Murarka, R., "Probabilistic Analysis and Design of a Retaining Wall, Journal of Geot. Div., ASCE, Vol. 100, GT3, pp.349-366, 1974.

22. Idriss, I.M., "Characteristics of Earthquake Ground Motions", Proc. ASCE Spec. Conf. on Earthquake Engin. and Soil Dynamics, Pasadena, CA, Vol. III, pp. 1151-1265, June 1978.

23. Lambe, T.W. and Whitman, R.V., Soil Mechanics, Wiley, N.Y., 1969.

24. Lumb, P., "Spatial Variability of Soil Properties", Proc. 2nd Int. Conf. Applic. of Stat. and Probab. in Soil and Struct. Engin., Aachen, W. Germany, pp. 397-422, 1975.

25. Lumb, P., "Precision and Accuracy of Soil Test", Proc. 1st Int. Conf. Applic. of Stat. and Probab. in Soil and Struct. Engin., Honk Kong, pp. 329-346, 1971.

26. Lumb, P., "Safety Factors and Probability Distribution of Soil Strength", Canadian Geot. Journal, Vol. 7, No. 3, pp. 225, 1970.

27. Lumb, P., "Variability of Natural Soils", Canadian Geot. Journal, Vol. 3, No. 2, pp. 74-97, 1966.

28. Matsuo M. and Kuroda, K., "Probabilistic Approach to Design of Embankments", Soils and Foundations, Japan, Soc. of Soil Mechan. and Found. Engin., Vol. 14, No. 2, pp. 1-17, June 1974.

29. Merz, H.A. and Cornell, C.A., "Seismic Risk Analysis Based on a Quadratic Magnitude - Frequency Law", Bull. of Seism. Soc. of Amer., Vol. 63, No. 6,pp. 1999-2006, 1973.

30. Newmark, N.M., "Effects of Earthquakes on Dams and Embankments", Fifth Rankine Lecture, Geotechnique, Vol. XV, No. 2, pp. 139-160, June 1965.

31. O'Rourke, M.J. and Solla. E., "Seismic Risk Analysis of Latham", SVBDUPS Report No. 3, Dept. of Civil Engineering, Rensselaer Polytechnic Institute, June 1977.

32. Papoulis, A., Probability Variables and Stochastic Processes, Mc-Graw-Hill, N.Y., 1965.

33. Rendulic, L., "Ein Beitrag zur Bestimmung der Gleitsicherheit", Der Bauingenieuz, No. 19/20, 1935.

34. Romani, F., Lovell, C.W. and Harr, M.E., "Influence of Progressive Failure on Slope Stability", Journal of the Soil Mech. and Found. Div. ASCE, Vol. 98, SM11, pp. 1209-1223, Nov., 1972.

35. Rosenblueth, E., "Point Estimates for Probability Moments", Proc. Nat. Acad. Sci, USA, Vol. 72, No. 10, pp. 3812-3814, October 1975.

36. Schreider, I.A., Monte Carlo Method, Pergamon Press, N.Y., 1966.

37. Schultze, E., "Frequency Distributions and Correlations of Soil Properties", Proc. 1st Inter. Conf. Applic. of Stat. and Probab. in Soil and Struct. Engin., Hong Kong, pp. 371-387, 1971.

38. Seed, B.H., "Slope Stability during Earthquakes", Journal of Soil Mechan. and Found. Div., ASCE, Vol. 43, SM4, pp. 329-357, July 1967.

39. Seed, H.B., "A Method for Earthquake-Resistant Design of Earth Dams", Journal of Soil Mech. and Found. Div., ASCE, Vol. 92, No. SM1, pp. 13-41, January 1966.

40. Singh, A. and Lee. K.L., "Variability of Soil Parameters", Proc. 8th Annual Symp. on Engin. Geology and Soils Engin., Idaho State Univ., 1970.

41. Tang, W.H., Yucemen, M.S. and Ang, A. H-S., "Reliability Analysis and Design of Braced Excavation", Proc. 1st Inter. Conf. Applic. of Stat. and Probab. in Soil and Struct. Engin., Hong Kong, pp. 187-202, 1971.

42. Tong, W.H., "Seismic Risk Analysis for Two-Sites Case", SDDA Report No. 18, Dept. of Civil Engineering, Massachusetts Institute of Technology, June 1975.

43. United States Nuclear Regulatory Commission Standard Review Plan, Section 3.7.1, Office of Nuclear Reactor Regulation, 1975.

44. Vanmarcke, E.H., "Reliability of Earth Slopes", Journal of the Geot. Div., ASCE, GT11, pp. 1247-1265, November 1977.

45. Vanmarcke, E.H., "Probabilistic Modeling of Soil Profiles", Journal of the Geot. Div., ASCE, GT11, pp. 1227-1246, November 1977.

46. Veneziano, D., "Probabilistic and Statistical Models for Seismic Risk Analysis", SDDA Report No. 21, Department of Civil Engineering, Massachusetts Institute of Technology, 1975.

47. Whitman, R.V., "Costs and Benefits of Providing Increased Seismic Resistance", Proc. Earthquake Engin. Conf., Univ. of S. Carol., January 1975.

48. Whitman, R.V., "Influence of Earthquakes on Stability", Proc. 1st Inter. Conf. on Stabil. of Open Pit Mining, Vancouver, B.C., Canada, pp. 23-25, Nov. 1970.

49. Wright, S.G., Kulhawy, F.H. and Duncan, J.M., "Accuracy of Equilibrium Slope Stability Analysis", Journal of Soil Mech. and Found. Div., ASCE, Vol. 99, No. SM10, pp. 783-791, 1973.

50. Wu, T.H. and Kraft, L.M., "Seismic Safety of Slopes", Journal of the Soil Mech. and Found. Div., ASCE, Vol. 96, No. SM2, pp. 609-629, March 1970.

51. Wu, T.H., "Uncertainty, Safety, and Decision in Soil Engineering Journal of the Geot. Div., ASCE, GT3, pp. 329-348, March 1974.

APPENDICES

APPENDIX A: DISTRIBUTION OF EARTHQUAKE MAGNITUDE FOR A LOG-QUADRATIC FREQUENCY-MAGNITUDE RELATIONSHIP

A general quadratic relationship between the logarithm of the number of earthquakes n_m exceeding a certain magnitude m and the magnitude m can be written in the following form:

$$\ln(n_m) = a + bm + cm^2 \tag{A-1}$$

where a, b, and c are regional parameters.

From Equation (A-1), one has

$$n_m = \exp(a + bm + cm^2). \tag{A-2}$$

If m_o and m_1 denote the lower and upper limit of m, respectively, Equation (A-1) may be written as

$$\ln(n_m) = a + b(m-m_o) + c(m-m_o)^2, \qquad m_o \leq m \leq m_1 \tag{A-3}$$

From Equation (A-2), one has that the expected number of earthquakes (n_{m_o}) with magnitude greater than the assumed lower bound (m_o) is equal to

$$n_{m_o} = \exp(a + bm_o + cm_o^2) \tag{A-4}$$

The ratio of n_m over n_{m_o} signifies the probability with which the earthquake magnitude is greater than m [42]; i.e.,

$$P[M > m] = \frac{n_m}{n_{m_o}} = \frac{\exp(a+bm+cm^2)}{\exp(a+bm_o+cm_o^2)} = \exp[b(m-m_o)+c(m^2-m_o^2)], m \geq m_o \quad \text{(A-5)}$$

The cumulative density function F(m) of the earthquake magnitude m is equal to

$$F(m) = P[M \leq m] = 1 - P[M > m]$$

Introducing Equation (A-5) in the above expression, one has

$$F(m) = 1 - \exp[b(m-m_o)+c(m^2-m_o^2)] \quad \text{(A-6)}$$

The normalizing factor k can be determined from the condition $F(m_1) = 1$; i.e.,

$$F(m_1) = k\{1 - \exp[b(m_1-m_o)+c(m_1^2-m_o^2)]\} = 1$$

or,

$$k = \{1-\exp[b(m_1-m_o) + c(m_1^2-m_o^2)]\}^{-1} \quad \text{(A-7)}$$

Thus, the cumulative density function for the earthquake magnitude is equal to

$$F(m) = \begin{cases} 0 & m < m_o \\ k\{1 - \exp[b(m-m_o) + c(m^2-m_o^2)]\} , & m_o \leq m \leq m_1 \\ 1 & m_1 < m \end{cases} \quad \text{(A-8)}$$

where k is given by Equation (A-7). The probability density function f(m) can again be formed by taking the derivative of F(m) with respect to m, i.e.,

$$f(m) = -k(b-2cm)\exp[b(m-m_o)+c(m^2-m_o^2)], \quad m_o < m < m_1 \qquad \text{(A-9)}$$

APPENDIX B: MAXIMUM ACCELERATION FOR THREE TYPES OF EARTHQUAKE SOURCES

(a) Point Source

For an attenuation relationship expressed in the form

$$a_{max} = b_1 e^{b_2 m} (R + b_4)^{-b_3}$$

the corresponding probability density function $f(a_{max})$ and range of variation of a_{max} were given by Equations (2-16) and (2-17), respectively. The cumulative distribution $F(a_{max})$ of a_{max} (i.e., the probability with which a_{max} receives values smaller than or equal to a certain value) can be obtained through a integration of Equation (2-16). Thus,

$$F(a_{max}) = k\{1-\exp[-\beta(\frac{1}{b_2} \ln \frac{a_{max}(R+b_4)^{b_3}}{b_1} - m_o)]\} \tag{B-1}$$

If the upper limit of the earthquake magnitude (m_1) is unrestricted (i.e., $m_1 = \infty$), Equation (B-1) receives the form

$$F(a_{max}) = 1 - (R+b_4)^{-\frac{b_3\beta}{b_2}} \left(\frac{a_{max}}{b_1}\right)^{-\frac{\beta}{b_2}} \exp(\beta m_o) \tag{B-2}$$

In the case of the log-quadratic frequency-magnitude relationship presented in Appendix A, the cumulative distribution of a_{max} is equal to

$$F(a_{max}) = k\{1-\exp[b(G-m_o)+c(G^2-m_o^2)]\} \tag{B-3}$$

where k is given by Equation (A-7), and

$$G = \frac{1}{b_2} \ln \frac{a_{max}(R+b_4)^{b_3}}{b_1}$$

The frequency distribution of a_{max} can be found by forming the derivative of Equation (B-3) with respect to a_{max}; i.e.,

$$f(a_{max}) = -\frac{k}{b_2}\frac{1}{a_{max}}(2cG+b)\exp[b(G-m_o)+c(G^2-m_o^2)] \qquad \text{(B-4)}$$

(b) <u>Line Source</u>

In the case of the line source, for the log-linear frequency-magnitude relationship and $\theta = 90°$ (Figure 11b), the cumulative distribution $F(a_{max})$ of the maximum acceleration a_{max} has the form

$$F(a_{max}) = 1-[(1-k)+k\exp(\beta m_o)\left(\frac{a_{max}}{b_1}\right)^{\frac{-\beta}{b_2}} \cdot I] \qquad \text{(B-5)}$$

where $k, \beta, m_o, b_1, b_2, b_3$ are defined as before,

$$I = \int_D^{r_o} \frac{2R}{\ell\sqrt{R^2-D^2}}(R)^{\frac{-b_3\beta}{b_2}} dR, \text{ and}$$

R, r_o, D and ℓ are shown in Figure 11b.

The probability density function of a_{max} can be found by forming the derivative of Equation (B-5) with respect to a_{max}; thus,

$$f(a_{max}) = \frac{k}{b_1} \quad \frac{\beta}{b_2} \quad I\ (\beta m_o)(\frac{a_{max}}{b_1})^{-(\frac{\beta}{b_2}+1)} \tag{B-6}$$

An alternative formulation of the line source, convenient for use is a Monte Carlo simulation scheme, is as follows:

Assuming that the earthquake has the same likelihood of occurrence at each point along the fault, a random number (RAN) can be used to determine the position of the source along the fault. Thus, for

$$x = RAN \cdot \ell, \qquad 0 \leq x \leq \ell$$

where ℓ is the length of the fault, the distance z between the center of the line and the simulated earthquake (Figure 11b) is equal to

$$z = (x - \ell/2), \ -\frac{\ell}{2} \leq z \leq \frac{\ell}{2}$$

Applying the cosine law, it is found that the distance R from the site to the simulated earthquake is equal to

$$R = [z^2 + D^2 - 2zD\cos(\theta)]^{1/2} \tag{B-7}$$

(c) Area Source

In the case of a log-linear frequency-magnitude relationship, the probability with which the maximum acceleration A_{max} receives values larger than a_{max} is equal to [42]

$$P[A_{max} > a_{max}] = (1-k) + \frac{2}{d^2-h^2} k[\exp(\beta m_o)]b_1^{\beta/b_2} H a_{max}^{-\beta/b_2} \quad \text{(B-8)}$$

where

$$H = \frac{h^{-\frac{b_3}{b_2}\beta+2}\left[1-(d/h)^{-\frac{b_3}{b_2}\beta+2}\right]}{\frac{b_3}{b_2}\beta-2}$$

b,h are defined in Figure 11c, and

β, b_1, b_2, b_3 are regional parameters.

The cumulative distribution $F(a_{max})$ of a_{max} can be obtained as the complement of Equation (B-8), i.e.,

$$F(a_{max}) = 1-[(1-k)+ \frac{2}{d^2-h^2} k \exp(\beta m_o) b_1^{\beta/b_2} H a_{max}^{-\beta/b_2}] \quad \text{(B-9)}$$

The frequency distribution $f(a_{max})$ can be found from Equation (B-9) by forming the derivative of $F(a_{max})$ with respect to a_{max}, or

$$f(a_{max}) = \frac{2k}{d^2-h^2} \cdot \frac{\beta}{b_2} \cdot b^{\beta/b_2} \cdot H \cdot \exp(\beta m_o) \cdot a_{max}^{-(\beta/b_2+1)} \quad \text{(B-10)}$$

A simpler formulation of the area source (equivalent to the one used in the case of the line source) can be achieved by considering the circular area as consisting of uniformly distributed point sources with a varying radius R_p. The value of R_p must be chosen so that the following expression is true:

$$(\text{Area}_p) = (\text{RAN})(\text{Area}_S)$$

or, $$\pi R_p^2 = (\text{RAN})(\pi R_s^2)$$

or, $$R_p^2 = (\text{RAN}) R_s^2 \tag{B-11}$$

where R_p = the distance from the site to the point source (a random variable),

R_S = the radius of the area source, and

RAN = a random number between 0 and 1.

From Equation (B-11), one has that R_p is equal to

$$R_p = \sqrt{\text{RAN}} \cdot R_S, \qquad 0 \leq R_p \leq R_S \tag{B-12}$$